AD-A148 772 STATUS REPORT ON ENVIRONMENT PROPAGATION AND SYSTEM MODELING FOR AN ELF/V.. (U) KAMAN TEMPO SANTA BARBARA CA R R RUTHERFORD ET AL. 28 JUN 83 KT-83-017(R) 1/1

UNCLASSIFIED DNA-TR-82-161 DNA001-82-C-0024 F/G 20/14 NL

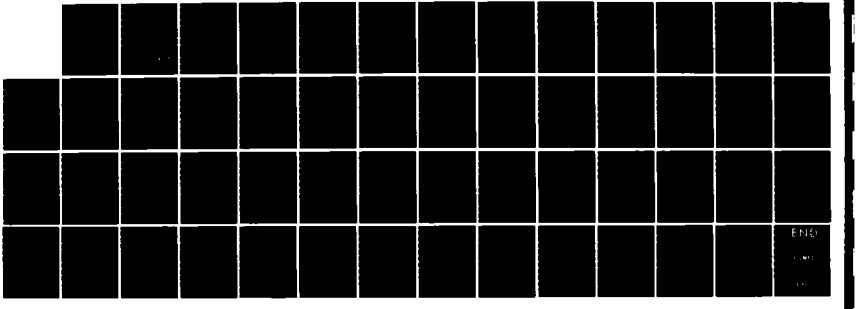

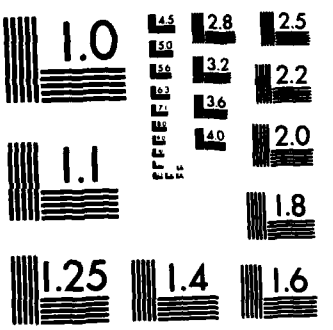

(12)

DNA-TR-82-161

STATUS REPORT ON ENVIRONMENT, PROPAGATION AND SYSTEM MODELING FOR AN ELF/VLF/LF IONOSPHERIC DEPENDENT PROPAGATION CODE

R. R. Rutherford
W. S. Knapp
Kaman Tempo
816 State Street
Santa Barbara, California 93102

28 June 1983

Technical Report

CONTRACT No. DNA 001-82-C-0024

THIS WORK WAS SPONSORED BY THE DEFENSE NUCLEAR AGENCY
UNDER RDT&E RMSS CODE X322083469 Q94QAXBC00001 H2590D.

Prepared for
Director
DEFENSE NUCLEAR AGENCY
Washington, DC 20305

Destroy this report when it is no longer needed. Do not return to sender.

PLEASE NOTIFY THE DEFENSE NUCLEAR AGENCY, ATTN: STTI, WASHINGTON, D.C. 20305, IF YOUR ADDRESS IS INCORRECT, IF YOU WISH TO BE DELETED FROM THE DISTRIBUTION LIST, OR IF THE ADDRESSEE IS NO LONGER EMPLOYED BY YOUR ORGANIZATION.

UNCLASSIFIED

SECURITY CLASSIFICATION OF THIS PAGE (When Data Entered)

REPORT DOCUMENTATION PAGE		READ INSTRUCTIONS BEFORE COMPLETING FORM
1. REPORT NUMBER DNA-TR-82-161	2. GOVT ACCESSION NO. AD-A148772	3. RECIPIENT'S CATALOG NUMBER
4. TITLE (and Subtitle) STATUS REPORT ON ENVIRONMENT, PROPAGATION AND SYSTEM MODELING FOR AN ELF/VLF/LF IONOSPHERIC DEPENDENT PROPAGATION CODE		5. TYPE OF REPORT & PERIOD COVERED Technical Report 6. PERFORMING ORG. REPORT NUMBER KT-83-017(R)
7. AUTHOR(s) Royden R. Rutherford Warren S. Knapp		8. CONTRACT OR GRANT NUMBER(s) DNA 001-82-C-0024
9. PERFORMING ORGANIZATION NAME AND ADDRESS Kaman Tempo 816 State Street Santa Barbara, California 93102		10. PROGRAM ELEMENT, PROJECT, TASK AREA & WORK UNIT NUMBERS Task Q94QAXBC-00001
11. CONTROLLING OFFICE NAME AND ADDRESS Director Defense Nuclear Agency Washington, DC 20305		12. REPORT DATE 28 June 1983 13. NUMBER OF PAGES 54
14. MONITORING AGENCY NAME & ADDRESS(if different from Controlling Office)		15. SECURITY CLASS. (of this report) UNCLASSIFIED 15a. DECLASSIFICATION/DOWNGRADING SCHEDULE N/A since UNCLASSIFIED

16. DISTRIBUTION STATEMENT (of this Report)

Approved for public release; distribution unlimited.

17. DISTRIBUTION STATEMENT (of the abstract entered in Block 20, if different from Report)

18. SUPPLEMENTARY NOTES

This work was sponsored by the Defense Nuclear Agency under RDT&E RMSS Code X322083469 Q94QAXBC00001 H2590D.

19. KEY WORDS (Continue on reverse side if necessary and identify by block number)

Longwave Propagation
ELF Propagation
VLF Propagation
LF Propagation
Nuclear Weapon Effects
Computer Codes

20. ABSTRACT (Continue on reverse side if necessary and identify by block number)

This report describes the continuing work on WEDCOM during the 1982 contractual period. Environmental models were updated and efficient propagation computational procedures were implemented to reduce execution time. Procedures were developed to provide the WEDCOM user with an automated method of selecting calculation times and ionization profile locations consistent with nuclear environmental sensitivities. VLF/LF signal processing models were adapted for use in WEDCOM and procedures for including atmospheric noise were developed.

DD FORM 1 JAN 73 1473 EDITION OF 1 NOV 68 IS OBSOLETE

UNCLASSIFIED

SECURITY CLASSIFICATION OF THIS PAGE (When Data Entered)

TABLE OF CONTENTS

TABLE OF CONTENTS (concluded)

LIST OF ILLUSTRATIONS

LIST OF TABLES

SECTION 1
INTRODUCTION

This report describes work on the WEDCOM environmental, propagation and system models performed during 1982. This effort is a continuation of work to prepare a revised version of WEDCOM, called WEDCOM V, by January 1984. The environmental and system modeling tasks are new. The propagation model tasks were concerned with the implementation and verification of the models developed during the previous effort, reported in Reference 1.

Section 2 describes work on the environmental models to incorporate current models and provide for code selection of calculation times and location of vertical ionization profiles along the propagation path.

Section 3 describes the implementation and modifications to the new VLF/LF propagation models described in Reference 1. The code structure was optimized to allow efficient computations consistent with the propagation sensitivities with the objective to reduce the link evaluation time required by WEDCOM IV. Significant computational time reductions were obtained, but they were case dependent. Computation time reductions achieved are typically factors of three to five for the VLF and LF models and five to ten for the ELF model. The actual time reduction is complicated by a new procedure which more accurately accounts for ionospheric and ground conductivity variations than did the WEDCOM IV code. The number of detailed reflection coefficient and diffraction computations may be greater than might have been specified by the WEDCOM IV user. However, the overall code efficiency and propagation parameter sensitivity has been improved.

The propagation model verification was accomplished by combining these models with the WEDCOM IV (Reference 2) structure and environmental models. A determination of model accuracy and computational time savings was made by comparisons with the WEDCOM IV code.

The new ELF propagation model implementation is described in Section 4. Comparisons to other models are made for model verification and the new subroutines are described.

VLF/LF system modem models developed by the Stanford Research Institute (References 3 and 4), were adapted for WEDCOM. This effort is described in Section 5. Also described is the work on an atmospheric noise model that includes the effects of a nuclear environment.

SECTION 2
ENVIRONMENTAL MODEL ADDITIONS

This section describes the following modifications to the WEDCOM code environmental models:

1. Implement current environmental modeling.
2. Provide for code-selected computational times.
3. Provide for code-selected vertical path locations.
4. Provide for ionization file retention for subsequent system computations.

IMPLEMENT CURRENT ENVIRONMENT MODELS

The environment models used in WEDCOM IV are those developed for WEPH IV Mod 2 in 1976 (Reference 5). The following revised environment models prepared for the WEPH code (Reference 6) and the WESCOM code (Reference 7) have been implemented into WEDCOM.

Model	Comments
Ambient Atmosphere	ROSCOE Optics Model
Ambient Ionosphere	Provides for variation with solar and geographic conditions
Atmospheric Chemistry	ROSCOE Optics Model 1978
Post-Stabilization Debris	Improved agreement between analytic and numerical models
High-Altitude Fireball Plume	New late-time fireball and debris models

CODE-SELECTED CALCULATION TIMES

The WEDCOM IV user must specify the calculation times to be used for system evaluation. This is satisfactory for users who have some familiarity with the intrinsic characteristics of nuclear environments and system responses. However, adequate time selection can be difficult, particularly for complex scenarios.

In WEDCOM V provision is being made for both user- and code-selected calculation times. For code selection the user specifies the time interval of interest and the code will select a set of evaluation times that take into account spatial and temporal considerations.

A simplified flow chart showing the times selected for phenomenology calculations are shown in Figure 1. The output is a phenomenological file for all evaluation times determined by phenomenology variations. This file provides the burst characteristics (location, regions, etc).

A time array (1, 30, 120, 300, 900, 1800, 3600 seconds and every hour thereafter) is defined beginning at each burst time. The phenomenology computations require little execution time when compared to that required by the ionization and propagation models. Thus, for a single burst the nuclear phenomenology characteristics are determined after every detonation at the above time intervals (within the time frame interval). For a multiburst case the evaluation times occur at the same time intervals after each subsequent burst, but do not include the evaluation times associated with prior bursts. The phenomenology characteristics are stored on file for use in determining vertical ionization profiles at selected locations between transmitter and receiver. To minimize the number of ionization and propagation calculations, calculation times for a burst that is determined to be unimportant (described below) are replaced with times selected for prior important bursts before determining the ionization environment.

CODE-SELECTED VERTICAL PATH LOCATIONS

In WEDCOM IV the ionization environment is computed for verticals equally spaced along the great circle path between transmitter and receiver. In many cases this procedure selects too many verticals in undisturbed regions and too few where nuclear disturbances are important. A new procedure has been developed that provides for code-selected vertical path locations that are determined on the basis of the disturbed environment.

The procedure is based on first determining the importance of the prompt and delayed radiation from each burst at vertical path locations.

A maximum range of effects, R_d, for every prompt or debris region is defined. A prompt region is not considered if the detonation altitude H_b is less than 25 km because the region is too small for propagation sensitivity studies.

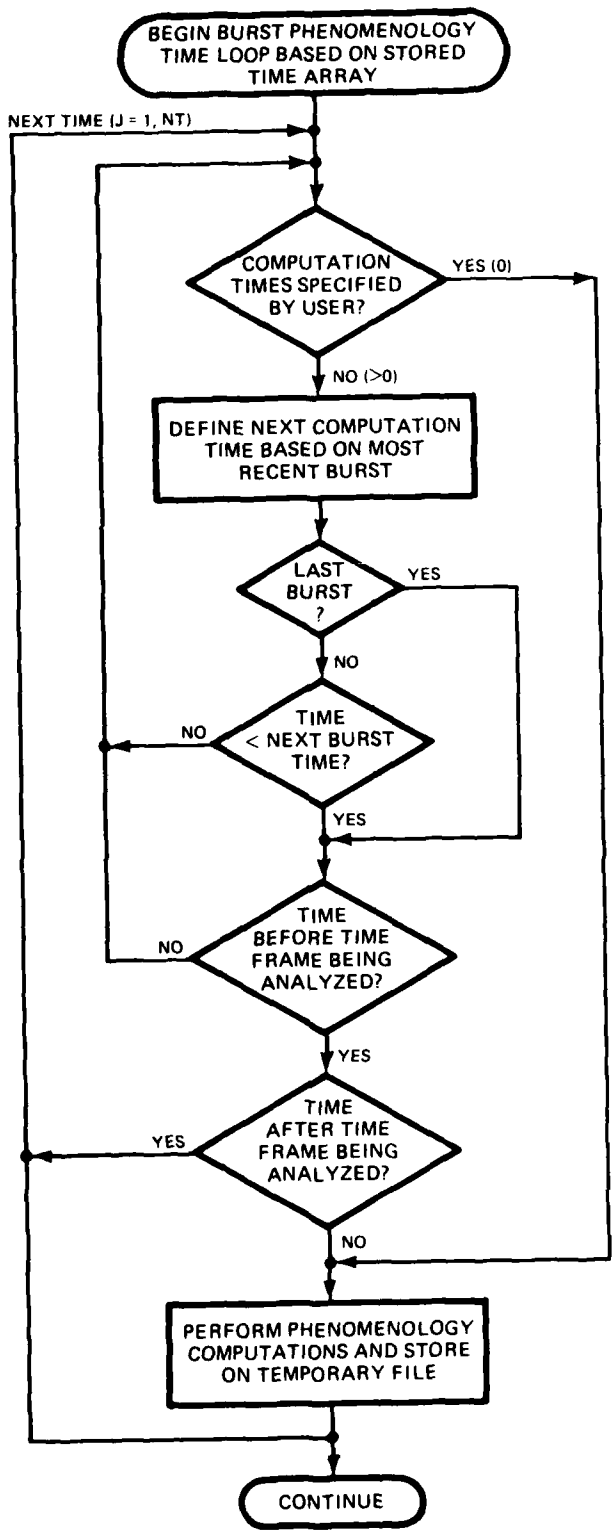

Figure 1. CONWED modifications illustrating the logic for selecting the initial computation times.

For higher detonation altitudes, R_d for prompt radiation is defined as

$$R_d = \begin{cases} 500 \text{ km}, & H_b < 85 \text{ km} \\ 500 + R_e \cos([R_e+85]/[R_e+H_b]) \text{ km}, & H_b > 85 \text{ km} \end{cases} \quad (1)$$

where R_e is the earth's radius.

A debris region is not considered if the debris altitude, H_d, is below 15 km. This elimination is also due to negligible propagation sensitivity. For higher debris altitudes, R_d is defined as

$$R_d = \begin{cases} R_{1d} + 25\ H_d - 375 \text{ km}, & \text{for } H_d < 25 \text{ km} \\ R_{1d} \operatorname{acos}([R_e+25]/[R_e+H_d]) + R_{1d} + 250 \text{ km}, & \text{for } H_d > 25 \text{ km} . \end{cases} \quad (2)$$

where R_{1d} is the radius of the debris.

A simplified flow chart for the vertical path selection is shown in Figure 2. Beginning at the transmitter, the propagation path is incremented toward the receiver (nominally in 500-km steps). At each segment location the range to the prompt source or debris center is determined. If this range is smaller than R_d, the segment and phenomenological time are flagged. A new phenomenology file is written (for up to twenty flagged evaluation times) which will subsequently be utilized for ionization calculations.

Once the segments have been flagged, logical tests are made to determine if at least two adjacent segments are flagged at a given evaluation time. If not, the single segment is ignored because the affected region is small and assumed to be negligible. However, if there are two or more adjacent flagged segments, the neighboring segments are flagged. This will help refine the disturbed region definition along the propagation path.

RETENTION OF IONIZATION FILE

If the time frame specified by the user is large compared to the time for signficiant environmental variations, the number of evaluation times selected by the code may be excessive, in turn requiring long and unacceptable computation times. The ionization file prepared by a WEDCOM execution will be retained to be

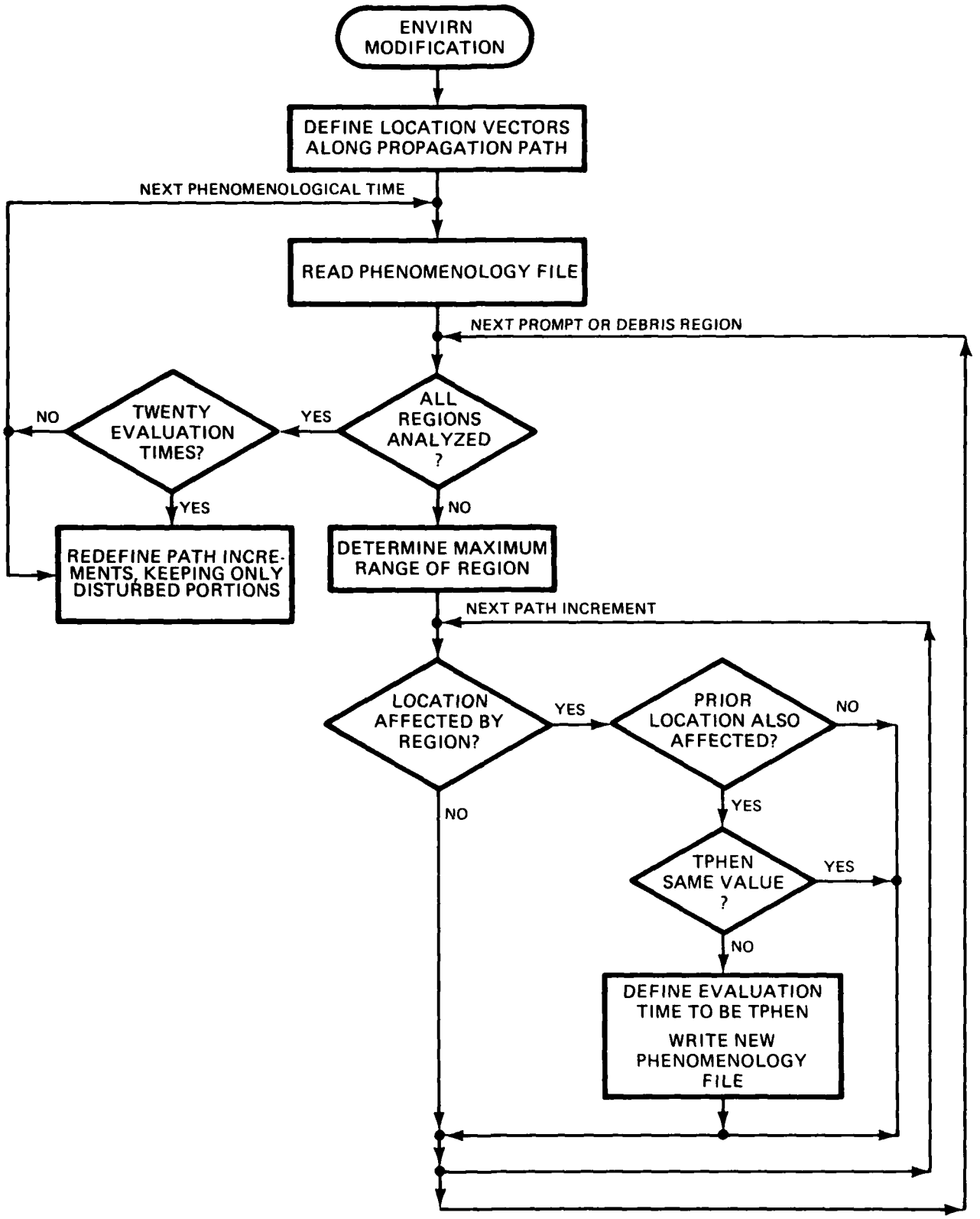

Figure 2. Logical flow implemented in Subroutine ENVIRN to determine computation locations.

utilized by a subsequent execution. Reference 1 suggests that this file be used to determine the ionization (by interpolation) at the user specified times. This feature, while straightforward to implement, would require significant new coding. Thus we have elected not to include it and to require the user to select from the preselected computation times.

The ionization file might have a large number of evaluation times, and while these times may represent the environment sensitivities they do not necessarily correspond to the propagation or system sensitivities. It is planned to require that the initial execution provide output such as ionospheric absorption, reflection altitudes, and gradients for the systems being analyzed. These outputs require minimal computation resources and would assist the user in selecting evaluation times for a subsequent execution.

SECTION 3
VLF/LF PROPAGATION MODEL IMPROVEMENTS

The effort reported here consists of the modification, implementation, and testing of the model techniques described in Reference 1. Changes and improvements were made in the overall structure of VLF and LF computations and in various submodels in both the LF and VLF model. Some of the modeling changes apply to both VLF and LF models. The following subsections will parallel the topics described in Sections 2, 3, and 4, Reference 1.

LF MODEL FORMULATION

This formulation was implemented as described in Subsection 2.2, Reference 1. Figure 3 illustrates the logical flow in Subroutine BHRHS which defines the ionospheric profiles at points along the propagation path. The profiles differ from one another by the ionization value and/or the magnetic propagation azimuth and dip angle. The profiles apply to path segments approximately equal to the spacing between profiles.

Reflection altitudes for the segments are not linearly interpolated between adjacent profiles as suggested in Reference 1, and as was done in past WEDCOM versions. Studies of a variety of reflection regions suggested that the interpolated values did not necessarily provide more accurate modeling. Therefore, a uniform reflection altitude corresponding to the profile at the segment center is used for each segment. This minimizes the number of reflection coefficient computations and reduces the amount of programming.

The complex-valued coefficients for the analytic ionospheric reflection coefficient formulation are computed as described in Section 3, Reference 1 and illustrated in Figure 4. Note that a maximum of three calls to the reflection coefficient model are made. The incident angle difference between the most oblique and steepest incident angles for each segment must be greater than 0.5 degrees to require two computations, and greater than 3 degrees to require three computations. Otherwise a single computation is performed.

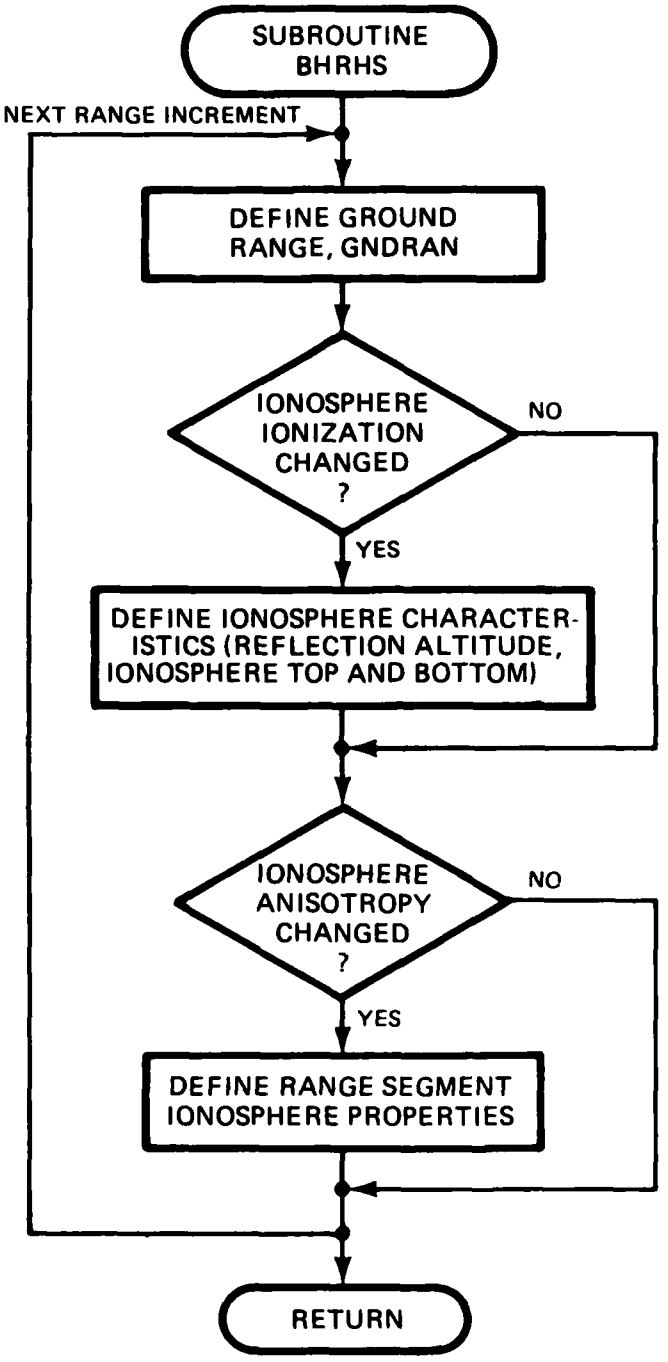

Figure 3. Logical flow for defining ionospheric segments along the propagation path.

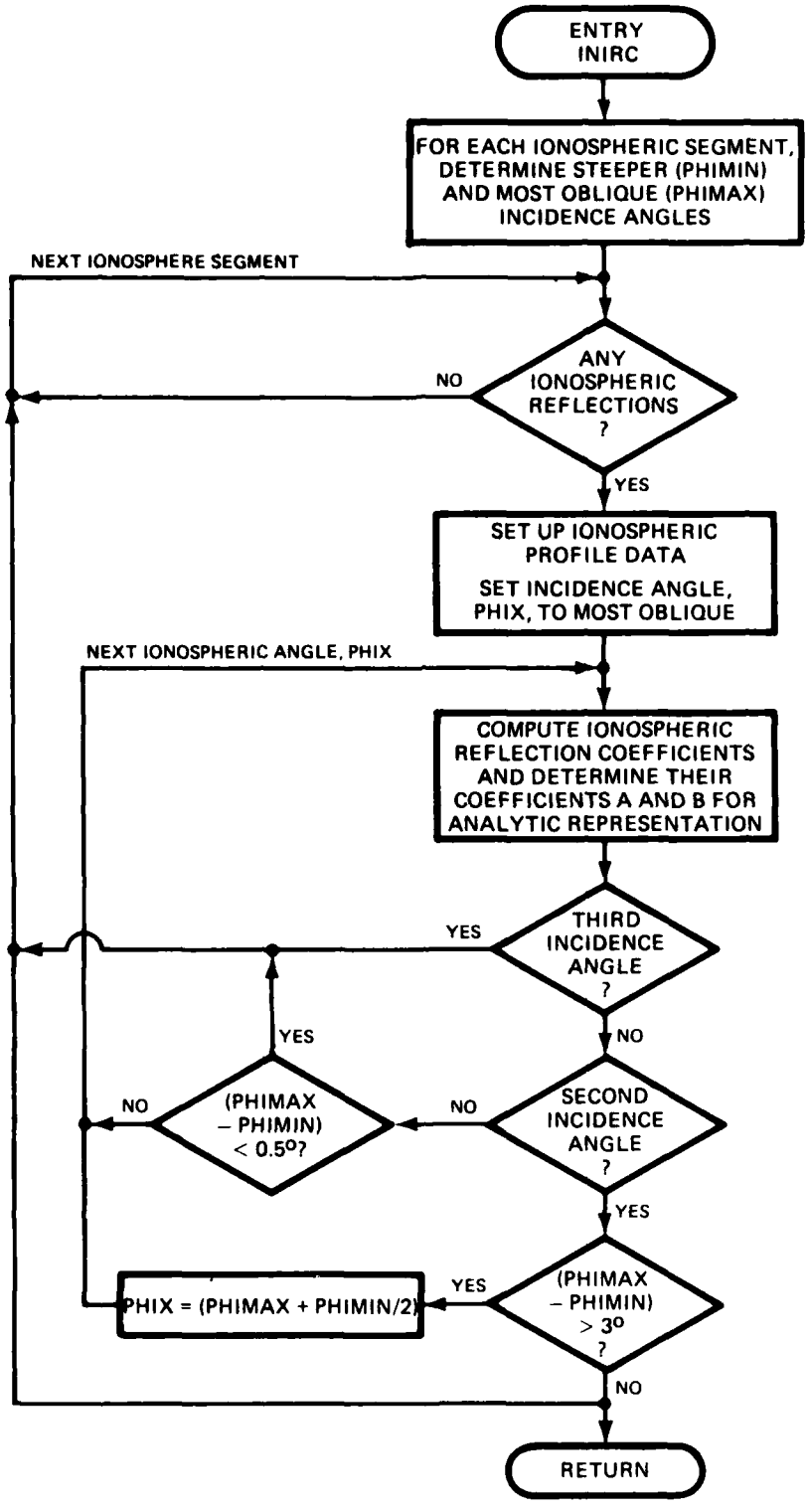

Figure 4. Logical flow for computing the complex-valued A and B coefficients for the analytic reflection coefficient formulation used in the LF model.

Sky Wave Calculations

Section 2.4, Reference 1, described the algorithms for the sky wave calculations. The earth-detached (Whispering Gallery) ray paths were also described. These are ray paths that propagate from one ionospheric reflection point to another without an earth reflection, and they can be very important for highly elevated antennas. However, the application of WEDCOM seldom requires antenna altitudes above that of normal aircraft; thus earth-detached ray-path model is not required and was not included. This omission insures computation time requirements consistent with the objectives of WEDCOM. There are special considerations for highly elevated antennas that are not easily incorporated into WEDCOM, especially for disturbed environments. Thus, WEDCOM V will simply output a flag noting that a user has specified an antenna altitude greater than 10 km.

Ground Wave/Earth Surface Diffraction

Sections 2.5 and 2.6, Reference 1, described the new ground wave and earth surface diffraction models for WEDCOM V implementation. These models are major users of computation time, second only to the ionospheric reflection coefficient model. Repetitive computations were eliminated from the model, as reported in Reference 1. Further reductions in repetitive computations were possible by utilizing the model characteristic that a maximum of six possible conductivities can be output from the worldwide ground conductivity map (see Section 2.3, Reference 1). Thus, the WEDCOM V code initializes the ground wave/diffraction models a maximum of six times, depending on the conductivity of segments of the propagation path.

Reflection Altitude

An analytic reflection altitude algorithm was outlined in Section 3.2, Reference 1. The requirement of an analytical formulation is essential to WEDCOM, but use of this formulation has shown some unusual reflection altitudes that may not be appropriate. Further study is in progress.

Reflection Coefficient Computation Criteria for Adjacent Vertical Ionospheric Profile

Section 3.3, Reference 1, described a criterion for determining reflection coefficient sensitivity to changes in the earth's magnetic field. For the vast majority of executions this criterion has worked well in minimizing the number of

reflection coefficient computations. However, for some lightly disturbed nighttime cases it has overestimated reflection coefficient sensitivities and led to too many computations. This algorithm is presently under study for the final WEDCOM V implementation.

Reflection Coefficient Interpolation Algorithm

The analytic reflection coefficient representation described in Section 3.4, Reference 1, estimates the reflection coefficient using

$$r_i = \exp \{A + BC_i\} \qquad (3)$$

where C_i is the cosine of the ionospheric angle of incidence and A and B are the complex constants computed in routine BHRHS, Figure 3. This procedure has proven very reliable for interpolating on ionospheric incident angle for most environmental simulations. It unexpectedly performed very well for anisotropic reflection and as well as expected for isotropic conditions. This formulation resulted in poor estimates of reflection coefficients for frequencies greater than 200 kHz and for VLF cases when reflection/absorption occurred over a thick altitude region. The first problem area is not serious since most cases of interest are below 200 kHz. The second problem area is more serious, resulting in inaccurate eigenangles. The problem is that Equation 3 is not adequate for the simplified eigenangle algorithm. The solution to this difficulty is described later.

VLF MODEL FORMULATION

The reflection coefficient computation criteria for adjacent vertical profiles, described under the LF model, also is used for VLF, with appropriate frequency dependence. The reflection coefficient interpolation algorithm also applies to both the LF and VLF models, but with some special modifications for VLF. The following subsections summarize submodel development which applies only to the VLF model.

Procedure to Reduce the Number of VLF Reflection Coefficient Computations

WEDCOM employs a modified version of MODESRCH, an eigenangle determination algorithm developed by NOSC and described in Reference 8. Section 4.2, Reference 1, described how the required number of ionospheric reflection coefficient

computations could be reduced by 25 to 50 percent compared to WEDCOM IV. A further reduction in the number of ionospheric reflection coefficients was obtained by first computing reflection coefficients using Equation 3 rather than for each corner of the complex-plane area being searched. The reflection coefficients are computed at complex ionospheric incident angles with real part defined by $Re(\theta_i)$ = 83, 81, 79, 77, 75 degrees, and imaginary part, $Im(\theta_i)$, that results in one dB attenuation for the corresponding value of $Re(\theta_i)$. The real and imaginary pairs are illustrated in Figure 5. The remainder of the modified MODESRCH procedure remains identical to that described for WEDCOM IV in Reference 2.

Eigenvalue Determination Using Analytic Reflection Coefficient Formulation and Initial Eigenangle Estimates

The initial eigenangle approximation algorithms described in Section 4, Reference 1, were implemented and tested for the matrix of cases shown in Table 1. The 280-degree azimuth and 30-degree dip angle correspond to strong anisotropic conditions. As mentioned earlier, the algorithm worked very well for the majority

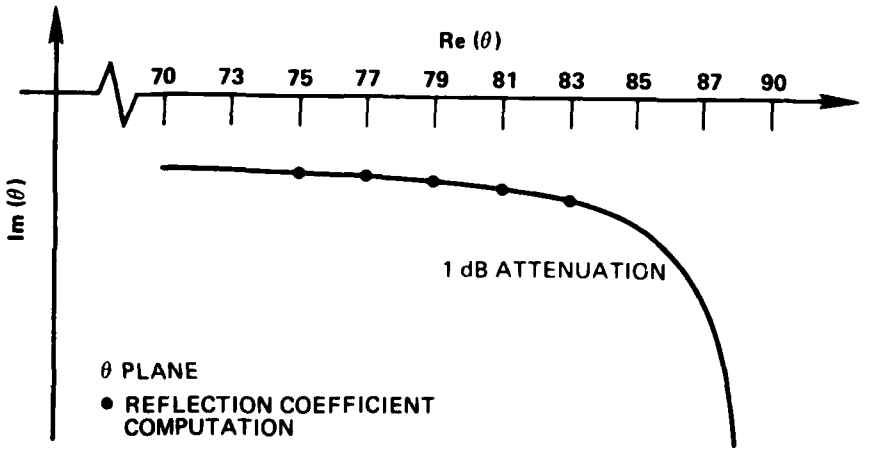

Figure 5. Illustrating the location of θ_i used for reflection coefficient computations.

Table 1. Parameters varied to test analytic eigenangle determinations.

Frequency	=	10, 15, 20, 25, 30 kHz
Azimuth	=	280 degrees
Dip	=	30, 70 degrees
Profiles	=	Normal day and night spread debris parameter $4 \times 10^{-(20, 11, 10, 9, 8, 7, 6, 5, 4)}$
Ground Conductivity	=	0.001, 0.01, 5.0 mho

of cases including highly anisotropic profiles. However, where the analytic reflection coefficient formulation (Equation 3) was not adequate, a few important eigenangles were not correctly computed. Several procedures were attempted to improve the eigenvalue approximations. The improvements were partially successful and show promise of complete success. If time permits these procedures will be pursued on the present effort as the computational time reduction and simpler coding makes this analytic formulation more desirable for WEDCOM than the search technique. If the approximation can't be completed, a brute force application of the MODESRCH technique will be implemented for these questionable cases.

Mode Conversion vs WKB

The use of mode conversion provides more accurate answers than the WKB approximation (an averaging technique), when propagation conditions vary in the direction of propagation. It also eliminates the need for defining an unambiguous mode numbering system. However, mode conversion requires more computation time than WKB. For this reason several near-uniform ionospheric profile cases were run using both the mode conversion and WKB procedures for computing field strengths as a function of range. The comparisons indicated that the computationally faster WKB procedure could be utilized for propagation paths with small variation in ground conductivity and ionospheric profile in the direction of propagation. The use of WKB when appropriate has been implemented.

SECTION 4
ELF PROPAGATION MODEL

A new ELF propagation model for the WEDCOM code was described in Reference 1. The model was adapted from a model developed by Booker (Reference 9) and is five to ten times faster running than the current WEDCOM model. Except for certain nighttime ambient ionospheres noted in Reference 1 the new model appears to give acceptable accuracy for cases of interest. In the following, model changes to improve results for ambient nighttime ionospheres and procedures used to implement the new model into the WEDCOM code are described.

REFLECTION FOR AMBIENT NIGHTTIME CONDITIONS

Tables 2 through 5 show phase velocity, c/v, and attenuation rate, α , obtained with the Booker and NOSC (full-wave solution) models for ambient nighttime profiles (References 9 and 10). Tables 6 and 7 show the electron density, positive ion density, and collision frequencies used in the two nighttime models. As noted in Reference 1 the results are in good agreement for the nighttime profiles used by Booker but show differences in α of as much as a factor of two for the NOSC nighttime profile. The problem is related to the electron density used in the E-region. The NOSC profile differs from that used by Booker in that the E-region electron density minimum is too large to cause reflection of the extraordinary (X) wave in the Booker propagation model and the X wave energy reaching the E region is not returned (thus increasing α). Full-wave solutions performed at NOSC (Reference 10) and at Tempo show that considerable energy is returned from the region between 95 and 135 km. The calculation also shows strong coupling between the ordinary (O) wave and the X wave in the E-region. In order to include the energy reflected from the E-region for nighttime conditions the following additional computational steps have been added to those described in Reference 1.

Table 2. c/v and α obtained with Booker model for the Booker quiet night profile.

Frequency (Hz)	Latitude (deg)						
	10	20	30	45	60	75	85
75	1.34	1.13	1.12	1.12	1.13	1.13	1.13
	0.45	0.50	0.52	0.52	0.51	0.50	0.50
300	1.10	1.10	1.11	1.11	1.11	1.10	1.10
	2.20	3.37	3.84	3.98	3.99	3.77	3.69

Table 3. c/v and α obtained with Booker model for the NOSC quiet night profile.

Frequency (Hz)	Latitude (deg)						
	10	20	30	45	60	75	85
75	1.18	1.21	1.22	1.22	1.21	1.20	1.20
	1.38	1.27	1.35	1.44	1.65	1.81	1.86
300	1.13	1.14	1.15	1.15	1.16	1.16	1.16
	4.07	5.09	5.31	5.63	4.56	4.52	4.51

Table 4. c/v and α obtained with NOSC program for the Booker quiet night profile.

Frequency (Hz)	Latitude (deg)						
	10	20	30	45	60	75	85
75	1.13	1.13	1.12	1.12	1.13	1.13	1.13
	0.38	0.37	0.37	0.37	0.36	0.35	0.35
300	1.09	1.07	1.09	1.08	1.07	1.07	1.07
	1.05	3.06	4.77	4.88	4.05	3.39	3.21

Table 5. c/v and α obtained with NOSC program for the NOSC quiet night profile.

Frequency (Hz)	Latitude (deg)						
	10	20	30	45	60	75	85
75	1.17	1.19	1.19	1.18	1.17	1.16	1.16
	0.94	0.82	0.75	0.80	0.88	0.84	0.97
300	1.13	1.15	1.16	1.17	1.17	1.17	1.17
	2.91	3.00	3.28	2.91	3.14	3.33	3.39

Table 6. Profiles used for comparisons with NOSC calculations.

Alt (km)	N_e (cm^{-3})	N_+ (cm^{-3})	ν_e (s)	ν_i (s)
0.00	1.99E-06	5.50E+03	4.30E+11	1.07E+10
5.00	3.35E-06	4.00E+03	1.90E+11	5.30E+09
10.00	6.83E-06	3.50E+03	8.50E+10	2.60E+09
15.00	1.55E-05	3.30E+03	3.77E+10	1.29E+09
20.00	3.54E-05	3.40E+03	1.66E+10	6.37E+08
25.00	8.45E-05	3.70E+03	7.45E+09	3.15E+08
30.00	1.95E-04	3.30E+03	3.30E+09	1.55E+08
35.00	4.00E-04	3.00E+03	1.47E+09	7.70E+07
40.00	7.67E-04	2.50E+03	6.50E+08	3.80E+07
45.00	2.05E-03	2.00E+03	2.70E+08	1.90E+07
50.00	4.98E-03	1.50E+03	1.30E+08	9.30E+06
55.00	1.23E-02	1.00E+03	5.70E+07	4.60E+06
60.00	3.21E-02	8.00E+02	2.60E+07	2.30E+06
65.00	5.57E-02	5.00E+02	1.13E+07	1.10E+06
70.00	8.95E-02	4.00E+02	5.00E+06	5.50E+05
75.00	5.00E+00	4.00E+02	2.20E+06	2.70E+05
80.00	7.50E+01	3.70E+02	9.96E+05	1.34E+05
85.00	1.60E+02	4.00E+02	4.40E+05	6.64E+04
90.00	3.30E+02	4.50E+02	1.97E+05	3.28E+04
95.00	6.00E+02	6.00E+02	8.70E+04	1.60E+04
100.00	2.00E+03	2.00E+03	3.90E+04	8.00E+03
105.00	1.80E+03	1.80E+03	2.60E+04	4.00E+03
110.00	1.40E+03	1.40E+03	1.80E+04	2.00E+03
115.00	8.00E+02	8.00E+02	1.04E+04	1.00E+03
120.00	6.00E+02	6.00E+02	1.00E+04	3.00E+02
130.00	3.70E+02	3.70E+02	4.00E+03	1.50E+02
140.00	2.80E+02	2.80E+02	2.50E+03	8.00E+01
160.00	2.70E+02	2.70E+02	6.00E+02	1.80E+01
180.00	4.50E+02	4.50E+02	1.70E+02	6.00E+00
200.00	1.00E+03	1.00E+03	4.50E+01	2.00E+00

Table 7. Booker nighttime profiles (60-degree latitude).

Alt (km)	N_e (cm^{-3})	N_+ (cm^{-3})	ν_e (s)	ν_i (s)
0.00	1.00E-08	3.15E+03	2.14E+12	3.39E+11
10.00	1.00E-08	3.14E+03	3.63E+11	5.75E+10
20.00	1.00E-08	3.09E+03	6.17E+10	9.77E+09
30.00	1.00E-08	2.79E+03	1.05E+10	1.66E+09
40.00	1.00E-08	1.91E+03	1.78E+09	2.82E+08
45.00	1.00E-08	1.40E+03	7.33E+08	1.16E+08
50.00	1.00E-08	9.93E+02	3.02E+08	4.79E+07
55.00	1.00E-08	7.03E+02	1.24E+08	1.97E+07
60.00	1.00E-08	5.11E+02	5.13E+07	8.13E+06
65.00	1.00E-08	3.93E+02	2.11E+07	3.35E+06
70.00	1.26E-05	3.17E+02	8.71E+06	1.38E+06
75.00	6.52E-02	2.47E+02	3.59E+06	5.69E+05
80.00	6.51E+01	2.21E+02	1.48E+06	2.34E+05
85.00	3.72E+02	4.37E+02	6.10E+05	9.66E+04
86.00	3.91E+02	4.42E+02	5.11E+05	8.09E+04
87.00	4.06E+02	4.45E+02	4.28E+05	6.78E+04
88.00	4.46E+02	4.75E+02	3.58E+05	5.68E+04
89.00	6.67E+02	6.89E+02	3.00E+05	4.75E+04
90.00	1.42E+03	1.44E+03	2.51E+05	3.98E+04
91.00	2.12E+03	2.13E+03	2.10E+05	3.33E+04
92.00	2.31E+03	2.32E+03	1.76E+05	2.79E+04
93.00	2.35E+03	2.36E+03	1.48E+05	2.34E+04
94.00	2.37E+03	2.37E+03	1.24E+05	1.96E+04
95.00	2.38E+03	2.39E+03	1.04E+05	1.64E+04
100.00	2.43E+03	2.43E+03	4.27E+04	6.76E+03
105.00	2.39E+03	2.39E+03	1.76E+04	2.79E+03
110.00	1.99E+03	1.99E+03	7.24E+03	1.15E+03
115.00	1.14E+03	1.14E+03	2.99E+03	4.73E+02
120.00	5.01E+02	5.01E+02	1.23E+03	1.95E+02
122.50	3.36E+02	3.36E+02	7.90E+02	1.25E+02
125.00	2.35E+02	2.38E+02	5.07E+02	8.04E+01
127.50	1.62E+02	1.62E+02	3.25E+02	5.16E+01
130.00	1.51E+02	1.51E+02	2.09E+02	3.31E+01
140.00	1.34E+02	1.34E+02	3.55E+01	5.62E+00
145.00	1.52E+02	1.52E+02	1.46E+01	2.32E+00
150.00	1.80E+02	1.80E+02	6.03E+00	9.55E-01
155.00	2.15E+02	2.15E+02	2.48E+00	3.94E-01
160.00	2.61E+02	2.61E+02	1.02E+00	1.62E-01
170.00	3.83E+02	3.83E+02	1.74E-01	2.75E-02
180.00	5.61E+02	5.61E+02	2.95E-02	4.69E-03
190.00	8.24E+02	8.24E+02	5.01E-03	7.94E-04
200.00	1.21E+03	1.21E+03	8.51E-04	1.35E-04

1. Determine the E-region altitudes where the real part of the extraordinary wave index of refraction reaches maximum and minimum values (near 100 and 140 km for the NOSC nighttime profiles).
2. Compute the equivalent height of reflection, Z_{RX} , for the extraordinary wave for reflection heights occurring below 100 km and for E-region reflection heights determined in Step 1. The phase change up to the bottom E-region reflection height is taken as the phase change up to the bottom altitude plus 0.63 percent of the phase change between the E-region altitudes determined in Step 1.
3. For cases where the Booker model does not result in reflections above 100 km the value of Z_{RX} determined in Step 2 is used to compute the phase velocity and attenuation rate. When the Booker model results in reflection above 100 km the attenuation rate is computed by the method defined in Step 2 and by methods as defined in the original model and the minimum attenuation rate and associated phase velocity are used.

Tables 8 and 9 show results obtained with the modified model for the two nighttime profiles. The modification does improve the results for the NOSC profile and either does not change or slightly improves the results for the Booker profile.

GROUND LOSSES

In the Booker model the earth is taken as a perfect conductor and ground losses are neglected. Ground losses can be added linearly to ionospheric losses as described by Wait (Reference 11)

$$\alpha = \frac{1}{2H_R}\left[\frac{Q}{N} + \frac{1}{N_g}\right] \quad \text{nepers km}^{-1}$$

where

α = attenuation rate

$\frac{Q}{N}$ = ionospheric loss term

N_g = ground complex index of refraction

H_R = effective reflection height (km).

Table 8. c/v and α obtained with revised Booker model for the Booker quiet night profile.

Frequency (Hz)	Latitude (deg)						
	10	20	30	45	60	75	85
75	1.14	1.13	1.13	1.13	1.13	1.13	1.13
	0.39	0.43	0.44	0.44	0.44	0.44	0.44
300	1.08	1.10	1.11	1.11	1.10	1.10	1.10
	1.63	3.37	3.84	3.98	3.98	3.77	3.69

Table 9. c/v and α obtained with revised Booker model for the NOSC quiet night profile.

Frequency (Hz)	Latitude (deg)						
	10	20	30	45	60	75	85
75	1.18	1.22	1.21	1.20	1.20	1.19	1.19
	1.38	0.83	0.86	0.94	1.02	1.07	1.09
300	1.11	1.15	1.11	1.15	1.19	1.18	1.18
	3.11	3.29	3.86	5.63	3.87	3.50	3.42

In terms of dB per Mm the ground loss term, dB_g, can be approximated by

$$dB_g \simeq \frac{8.7 \times 10^3}{2H_R} \sqrt{\frac{8.8 \times 10^{-12} \pi f}{\sigma}} \quad dB/Mm$$

where

f = propagation frequency (Hz)

σ = ground conductivity (mho m^{-1}).

IMPLEMENTATION OF BOOKER MODEL INTO THE WEDCOM CODE

Computer Routines

The following routines are used to implement the Booker model into the WEDCOM code.

Routine ACCUMB

This routine integrates a complex function f(x) for a specified interval in x assuming either a linear or exponential variation with x. Inputs to the routine are the values of the function at two values of x. The integral of the real and imaginary parts of the function are performed separately. If the value

of the real or imaginary part of the function changes by a factor of 2 or less a linear variation of the function is assumed; otherwise an exponential variation is assumed.

Routine BFZ

This routine computes a function used in the Booker interpolation scheme to provide smoothing at transition altitudes (Equation 48 in Reference 1).

Routine BKRIAC

This routine interpolates a function of the complex index of refraction using a four-point interpolation procedure. The derivative of the function can also be determined.

The four-point interpolation procedure based on the multiregion fitting technique of Booker is used to interpolate the function n^2-1 (see Equations 48 through 51 in Reference 1). Inputs are then $\ell n\ (|A|)$ and $\ell n\ (|B|)$ at four altitudes where A and B are the real and imaginary parts of the function. The signs of the real and imaginary parts of the interpolated value are negative for the ordinary wave and positive and negative respectively for the extraordinary wave. The wave type is determined from the input MWAVE (0 = ordinary, 1 = extraordinary). If the derivative of the function is requested (input IDER > 0), it is obtained by evaluating Equation 51 in Reference 1.

Routine BKRIAD

This routine interpolates a real function using a four-point interpolation procedure. The derivative of the function can also be determined.

Inputs to the routine are either the function or the log of the function at four points and the output is either the interpolated value or the log of the interpolated value. The four-point interpolation procedure based on the multiregion fitting technique of Booker is used to interpolate the function (see Equations 48 through 51 in Reference 1). If the derivative of the function is requested (input IDER > 0) it is obtained by evaluating Equation 51 in Reference 1.

Routine BOKELF

This routine computes the complex propagation constant at a specified location using approximations developed by Booker. A simplified flow chart for the routine is shown in Figure 6.

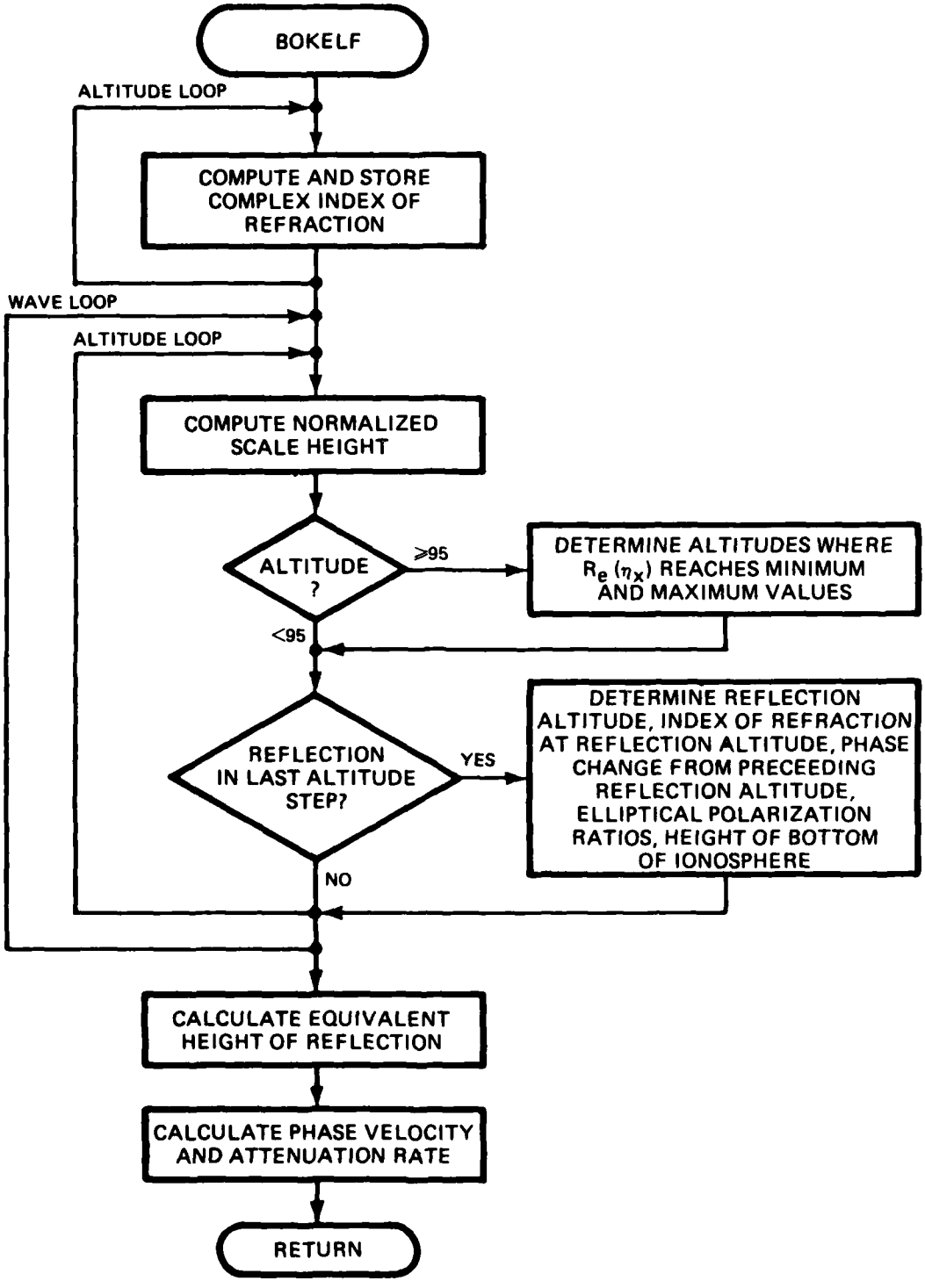

Figure 6. Simplified flow chart for routine BOKELF.

First, the complex index of refraction (n) is computed at each altitude and the results (actually n^2-1) stored by calling routine RIQT. For daytime conditions calculations are only made at and below 100 km. Next, a wave loop is established to perform calculations for the ordinary wave (MODEP=0) and the extraordinary wave (MODEP=1). For each wave the index of refraction is determined at each altitude by calling routine BKRIAC. This routine determines the index of refraction using a four-point fit to the previously stored values that insures continuous derivatives. The index of refraction quantities are used to determine the ratio of the local wavelength to the refractive index local scale height. For altitudes above 95 km the altitudes where the real part of the index of refraction for the extraordinary wave reaches maximum and minimum values are determined (used in computing E-region reflection of the extraordinary wave). Then, a test is made to determine whether there is a reflection altitude in the last altitude interval. The test depends on the reflection altitude number and the wave type as described in Reference 1.

If there is a reflection altitude within the interval the reflection altitude is computed. An iterative procedure is used to account for the change in reflection criteria with index of refraction. After the reflection altitude is determined, routine BKRIAD is called to determine ionization and collision frequency values at the reflection altitude and routine RIQT is called to determine the complex index of refraction. The polarization ratios are computed (Equation 36, Reference 1) and the phase change between reflection heights determined (Equations 40 through 43, Reference 1). For the first reflection height the equivalent height of the bottom of the ionosphere is computed (Equation 44, Reference 1). In computing the bottom altitude for the ordinary wave tests are made to see if the real part of the index of refraction goes to zero. If it does, the height where it goes to zero is determined and used in computing the bottom altitude.

After the reflection heights and other quantities have been computed for both the ordinary and extraordinary waves the equivalent height of reflection is computed (Equation 39, Reference 1). For nighttime conditions the additional steps described in this report are used to account for nighttime profiles where the extraordinary wave would not be reflected using the Booker criteria. Then the complex propagation constant is determined and used to evaluate the phase velocity and attenuation rate.

The mode solution is determined by calling routine BOKELF for vertical paths between the transmitter and receiver. Then ground losses are determined and the mode constant adjusted to include these losses. If the multiple receiver location option is exercised (KALCMR = 1), excitation and height gain factors are found for each vertical path on the short great circle path between transmitter and receiver. Otherwise, excitation and height gain factors are only found for the vertical paths at the transmitter and receiver terminals. If field strength calculations for propagation along both the short and long great circle paths are to be made, ground reflection coefficients and excitation factors at the transmitter and receiver terminals are computed for both propagation directions. The excitation and height gain factors for the long great circle path direction are not computed for receiver locations between the transmitter and receiver terminals specified in input.

Detailed output describing the eigenangle, attenuation rate, relative phase velocity, ionosphere reflection coefficients, ground reflection coefficients, and excitation factors are written out on the detailed output file if requested (input option). Finally, routine BOKTEM is called to evaluate the TEM mode field values at the receiver.

Routine BOKTEM

This routine calculates TEM mode field values at the receiver for ELF propagation. A simplified flow chart for the routine is shown in Figure 7.

First, propagation parameters and geometry are defined and nominal system output quantities are written out. Then a time loop over the calculation times is started and eigenvalue-dependent data parameters defined in routine ELFMOD are read from a data file. If ambient calculations have been requested (input option) data for ambient conditions are read in first; otherwise, data for disturbed conditions are obtained. The short path WKB approximation is always calculated and the long path calculation is made when requested (input option). Then the short path (and the long path when requested) electromagnetic fields at the receiver location are determined and nominal output is written out. If the multiple receiver location option (input option) has been exercised, the electromagnetic fields at each vertical path location are computed. After calculations have been completed for disturbed conditions, calculations are started for the next calculation time.

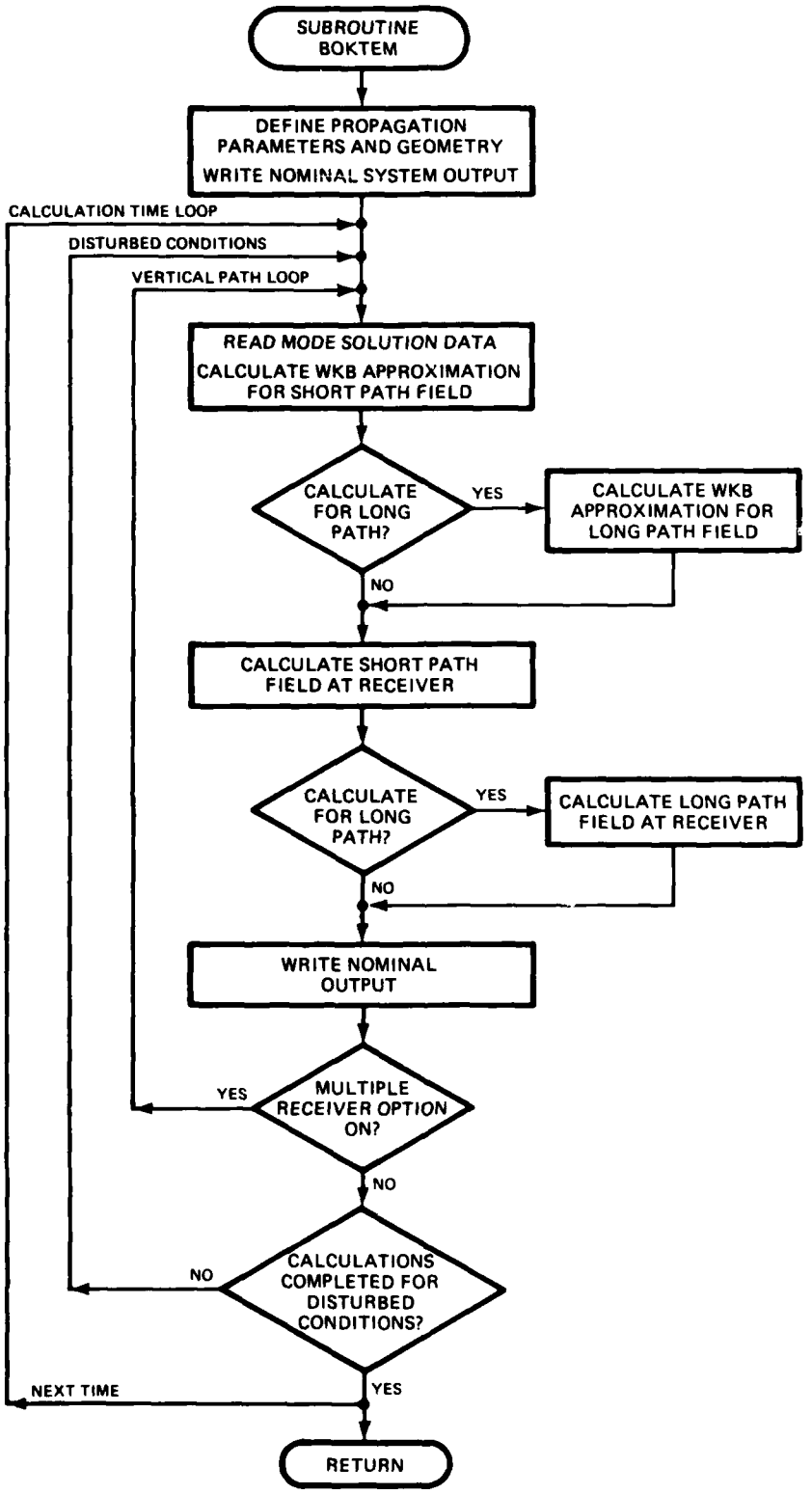

Figure 7. Simplified flow chart for routine BOKTEM.

Routine ELFMOD

This routine is the ELF propagation driver routine and determines anisotropic reflection coefficients, mode solutions, and excitation factors. Only the transverse electromagnetic wave is analyzed. A simplified flow chart for the routine is shown in Figure 8.

First reflection coefficients, excitation factors, and height gain parameters are initialized. Then a time loop over the calculation times is started and an ambient calculation flag (determines whether calculations will be made for ambient conditions) is set from input parameters.

Next a loop over the vertical paths between transmitter and receiver is started. For each path magnetic field and ground conductivity quantities are established and the level of detailed output requested determined. The ionization and collision frequencies along the vertical path for disturbed conditions are obtained from the environment file.

For ELF propagation there are NP-2 paths on the great circle between transmitter and receiver. When calculations are performed for long and short paths, only NPT2 paths are along the short path, the balance along the long paths. The last two paths (L = NP-1 and L = NP) are located a Fresnel zone distance normal to the short great circle path between transmitter and receiver and are used to determine whether the ionization normal to the great circle propagation path is spherically stratified (an assumption used in the propagation calculations). If the attenuation rate (dB per 1000 km) for either of the last paths is less than one half the attenuation rate at the path midpoint, a diffraction flag is set to indicate that the propagation calculations may be in error.

Routine RIQT

This routine determines the complex index of refraction at a point. The index of refraction (n) is computed (Equation 31, Reference 1) and the quantity n^2-1 is stored for the ordinary and extraordinary waves.

Routine SSQRT

This routine, obtained from the University of California, San Diego, determines the square root of a complex number with a consistent sign so that continuity in defining the ordinary and extraordinary waves is maintained over the entire altitude region of interest.

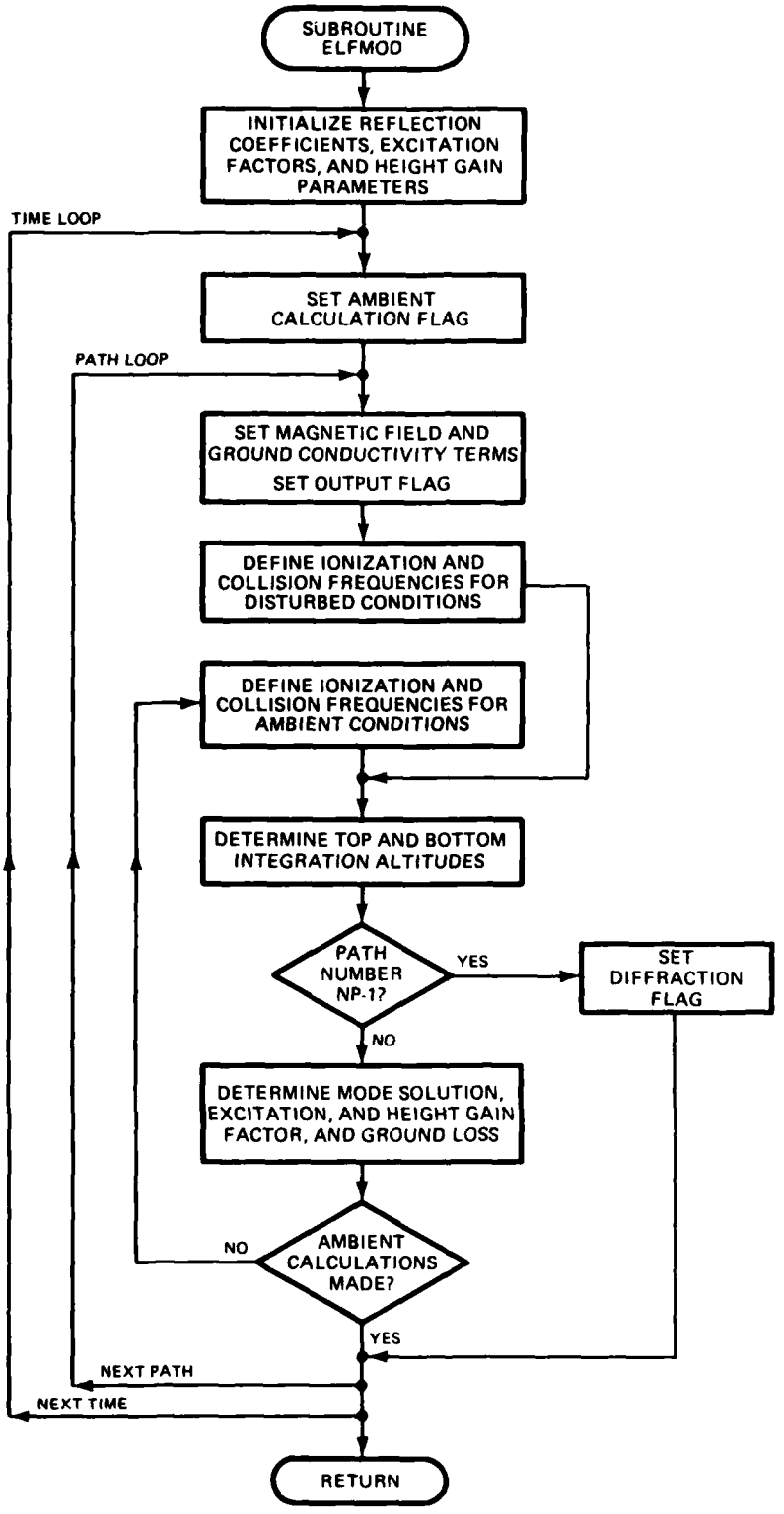

Figure 8. Simplified flow chart for routine ELFMOD.

WEDCOM Input and Output

Input to the WEDCOM code for ELF cases is the same with the new model as before except that the option to minimize reflection coefficient calculations is not used. Since the propagation constant calculations are much faster with the new model, it does not appear efficient to eliminate calculations.

Most of the output from the ELF model is identical to the previous model. Figures 9 and 10 show examples of detailed output from the old and new models respectively. For daytime conditions the maximum altitude considered is 100 km and detailed output for higher altitudes is not given. In the old model the index of refraction quantities are given at each altitude for a 90-degree magnetic dip angle (ordinary wave). The new model results show output for both the ordinary (O) and extraordinary (X) waves at the actual magnetic latitude of the profile.

An additional output, ATTENG, describing the ground loss in dB per 1000 km has been added to the detailed output and the ground reflection coefficients previously given have been deleted. Finally, height-gain factors are given with the excitation factors in the new model output.

```
VERTICAL PATH  3
   SIGMA        RELDC        DIP          M AZ         M FIELD      DAY OR
  (MHOS/M)                  (DEG)        (DEG)        (GAUSS)      NIGHT
  3.623E+00    5.907E+01    6.179E+01    2.379E+02    5.132E-01    DAY

DISTURBED IONOSPHERE PROFILE AND INDEX OF REFRACTION QUANTITIES
    ALT(KM)   ENE(CM-3)   ENP(CM-3)   XNUE(S-1)   XNUI(S-1)        A            B          REAL(N)      IMAG(N)
       0.00    7.55E-06    8.41E+03    9.17E+10    7.69E+09    2.13E-11    2.53E-04    1.00E+00    -1.27E-04
       5.00    1.83E-05    7.66E+03    4.91E+10    4.38E+09    5.93E-11    4.02E-04    1.00E+00    -2.01E-04
      10.00    4.69E-05    7.25E+03    2.40E+10    2.29E+09    2.08E-10    7.27E-04    1.00E+00    -3.64E-04
      15.00    9.42E-04    1.93E+04    1.11E+10    1.13E+09    2.49E-09    3.92E-03    1.00E+00    -1.96E-03
      20.00    1.53E-02    8.02E+04    5.01E+09    5.48E+08    7.64E-08    3.37E-02    1.00E+00    -1.68E-02
      25.00    1.91E-01    1.47E+05    2.30E+09    2.70E+08    2.04E-06    1.26E-01    1.00E+00    -6.29E-02
      30.00    7.09E-01    1.59E+05    1.09E+09    1.36E+08    3.79E-05    2.73E-01    1.01E+00    -1.35E-01
      35.00    3.13E+00    1.31E+05    5.29E+08    7.09E+07    6.86E-04    4.65E-01    1.03E+00    -2.27E-01
      40.00    2.44E+01    9.91E+04    2.66E+08    3.82E+07    2.10E-02    1.21E+00    1.13E+00    -5.39E-01
      45.00    7.76E+01    7.29E+04    1.38E+08    2.11E+07    2.49E-01    4.58E+00    1.64E+00    -1.39E+00
      50.00    1.57E+02    4.94E+04    7.26E+07    1.19E+07    1.79E+00    1.54E+01    2.70E+00    -2.84E+00
      55.00    7.90E+02    2.21E+04    3.84E+07    6.76E+06    3.10E+01    1.32E+02    7.27E+00    -9.11E+00
      60.00    1.66E+03    7.88E+03    1.99E+07    3.75E+06    2.14E+02    4.73E+02    1.24E+01    -1.91E+01
      65.00    2.48E+03    3.45E+03    9.92E+06    2.00E+06    8.39E+02    9.22E+02    1.43E+01    -3.23E+01
      70.00    2.52E+03    2.62E+03    4.68E+06    1.01E+06    1.49E+03    7.69E+02    9.68E+00    -3.97E+01
      75.00    2.50E+03    2.50E+03    2.06E+06    4.80E+05    1.78E+03    4.09E+02    4.82E+00    -4.24E+01
      80.00    3.05E+03    3.05E+03    8.79E+05    2.17E+05    2.26E+03    2.21E+02    2.33E+00    -4.76E+01
      85.00    5.76E+03    5.76E+03    3.62E+05    9.59E+04    4.30E+03    1.79E+02    1.37E+00    -6.96E+01
      90.00    1.36E+04    1.36E+04    1.49E+05    4.23E+04    1.01E+04    2.05E+02    1.02E+00    -1.01E+02
      95.00    3.77E+04    3.77E+04    6.30E+04    1.91E+04    2.82E+04    4.23E+02    1.26E+00    -1.68E+02
     100.00    1.00E+05    1.00E+05    2.76E+04    8.97E+03    7.49E+04    1.51E+03    2.75E+00    -2.74E+02
     105.00    1.95E+05    1.95E+05    6.63E+04    3.32E+03    1.47E+05    7.59E+03    9.90E+00    -3.83E+02
     110.00    2.40E+05    2.40E+05    4.20E+04    2.10E+03    1.83E+05    1.29E+04    1.50E+01    -4.28E+02
     115.00    2.21E+05    2.21E+05    1.66E+04    8.32E+02    1.80E+05    1.95E+04    2.29E+01    -4.24E+02
     120.00    2.39E+05    2.39E+05    1.01E+04    5.06E+02    2.05E+05    2.10E+04    2.32E+01    -4.53E+02
     130.00    3.05E+05    3.05E+05    7.32E+03    3.66E+02    2.69E+05    2.38E+04    2.29E+01    -5.19E+02
     140.00    2.49E+05    2.49E+05    2.80E+03    1.40E+02    2.29E+05    9.39E+03    9.81E+00    -4.79E+02
     160.00    3.05E+05    3.05E+05    9.82E+02    4.91E+01    2.83E+05    4.20E+03    3.95E+00    -5.32E+02
     180.00    3.70E+05    3.70E+05    1.56E+02    7.81E+00    3.43E+05    8.14E+02    6.95E-01    -5.85E+02
     200.00    1.48E+07    1.48E+07    6.94E+02    3.47E+01    1.37E+07    1.45E+05    1.95E+01    -3.71E+03
STARTING ALTITUDE=   94.7m          BOTTOM ALTITUDE=     0.00          REFERENCE ALTITUDE=     0.00

DISTURBED IONOSPHERE EIGEN VALUES AND REFLECTION COEFFICIENTS
DIRECTION      THETA (DEG)          SIN THETA          ATTEN       C/V
            REAL       IMAG      REAL       IMAG     (DB/1000)
  SPTH    7.54E+01  -4.78E+01  1.32E+00  -2.35E-01   3.21E+00   1.324085
            RVV                   RHH                  RHV                  RVH
         REAL       IMAG       REAL       IMAG       REAL       IMAG       REAL       IMAG
      1.00E+00  -2.50E-03  -1.20E+00   1.26E-01   2.02E-02   1.36E-02   2.01E-02   1.42E-02

SHORT PATH     GROUND REFLECTION COEFFICIENTS      EXCITATION FACTORS
                 REAL       IMAG        POLUR       REAL       IMAG        POLOR
               -1.00E+00   9.99E-05       VERT     2.80E+00   5.65E+00       VERT
               -1.00E+00   9.99E-05       HORZ    -1.32E+00  -4.50E+00        PAR
                                                  -3.68E-01   3.10E-01       NORM
```

Figure 9. Illustration of ELF detailed output for old model.

VERTICAL PATH 3

SIGMA (MHOS/M)	RELDC	DIP (DEG)	M AZ (DEG)	M FIELD (GAUSS)	DAY OR NIGHT
3.623E+00	5.907E+01	6.175E+01	2.379E+02	5.132E-01	DAY

DISTURBED IONOSPHERE PROFILE AND INDEX OF REFRACTION QUANTITIES

ALT(KM)	ENE(CM-3)	ENP(CM-3)	XNUE(S-1)	XNUI(S-1)	A	B	A	B
20.00	1.53E-02	8.02E+04	5.01E+09	5.48E+08	9.22E-08	3.71E-02	-2.83E-08	3.71E-02
25.00	1.51E-01	1.47E+05	2.30E+09	2.70E+08	1.77E-06	1.39E-01	-1.29E-06	1.39E-01
30.00	7.09E-01	1.59E+05	1.09E+09	1.36E+08	3.31E-05	3.01E-01	-3.11E-05	3.01E-01
35.00	3.13E+00	1.31E+05	5.29E+08	7.09E+07	6.00E-04	5.09E-01	-5.93E-04	5.09E-01
40.00	2.44E+01	9.91E+04	2.66E+08	3.82E+07	1.83E-02	1.28E+00	-1.83E-02	1.28E+00
45.00	7.76E+01	7.29E+04	1.38E+08	2.11E+07	2.17E-01	4.67E+00	-2.16E-01	4.67E+00
50.00	1.57E+02	4.94E+04	7.26E+07	1.19E+07	1.56E+00	1.55E+01	-1.56E+00	1.55E+01
55.00	7.90E+02	2.21E+04	3.84E+07	6.76E+06	2.72E+01	1.3 .+02	-2.72E+01	1.34E+02
60.00	1.68E+03	7.88E+03	1.99E+07	3.75E+06	1.94E+02	4.94E+02	-1.94E+02	4.94E+02
65.00	2.48E+03	3.45E+03	9.92E+06	2.00E+06	8.14E+02	1.04E+03	-8.14E+02	1.04E+03
70.00	2.52E+03	2.62E+03	4.68E+06	1.01E+06	1.61E+03	9.67E+02	-1.61E+03	9.68E+02
75.00	2.50E+03	2.50E+03	2.08E+06	4.80E+05	2.03E+03	5.45E+02	-2.03E+03	5.45E+02
80.00	3.05E+03	3.05E+03	8.79E+05	2.17E+05	2.63E+03	3.01E+02	-2.63E+03	3.01E+02
85.00	5.76E+03	5.76E+03	3.62E+05	9.59E+04	5.03E+03	2.45E+02	-5.03E+03	2.45E+02
90.00	1.36E+04	1.36E+04	1.49E+05	4.23E+04	1.19E+04	2.77E+02	-1.19E+04	2.77E+02
95.00	3.77E+04	3.77E+04	6.30E+04	1.91E+04	3.31E+04	5.58E+02	-3.31E+04	5.58E+02
100.00	1.00E+05	1.00E+05	2.76E+04	8.97E+03	8.82E+04	1.94E+03	-8.80E+04	1.93E+03

DISTURBED IONOSPHERE EIGEN VALUES

DIRECTION	THETA (DEG)		SIN THETA		ATTEN (DB/1000)	C/V	ATTENG (DB/1000)
	REAL	IMAG	REAL	IMAG			
SPTH	7.59E+01	-5.19E+01	1.40E+00	-2.52E-01	3.43E+00	1.395854	2.75E-03

SHORT PATH

EXCITATION FACTORS			HEIGHT GAIN FACTORS	
POLAR	REAL	IMAG	REAL	IMAG
VERT	6.17E+00	3.51E+00	2.00E+00	0.
PAR	3.21E+00	-3.84E+00	4.80E-05	4.80E-05
NORM	0.	0.	-3.14E-05	6.50E-05

Figure 10. Illustration of ELF detailed output for new model.

SECTION 5
ATMOSPHERIC NOISE AND SIGNAL PROCESSING MODELS

This section describes the preliminary work required to implement a signal processing capability into WEDCOM. Previous versions of WEDCOM computed signal propagation parameters such as the received EM field components or the signal-to-noise ratio (S/N). The atmospheric noise magnitude was specified by the user (using CCIR, Reference 12) and it was assumed that the received noise value was not modified by a nuclear environment. Estimates of message quality required additional processing not provided in WEDCOM. To be done properly, the message quality estimate requires knowledge of noise characteristics for both disturbed and undisturbed environments.

This additional processing required was awkward, especially for analysts with limited propagation and/or signal processing background. WEDCOM V will incorporate a signal processing model which includes noise sensitivity to nuclear environments.

ATMOSPHERIC NOISE MODEL

To provide useful data the noise model must define the characteristics of the received noise. Atmospheric noise for the lower frequencies is characteristically a homogeneous background superimposed with large, intermittent, nonoverlapping, pulses. The noise is due to thunderstorm activity, and the large spikes result from local lightning strikes. The homogeneous background is due to numerous unresolvable pulses from distant sources, where the pulses are stretched in time due to propagation dispersion.

The atmospheric noise can be characterized as received noise from a few transmitter (noise source) locations. This assumption is especially good for receiver modems located somewhat distant from the noise sources. For example, Figure 11 illustrates that the centroids of the noise sources tend to be centered south of the equator during the winter season. For this case the background noise for receivers located in CONUS could be modeled by a single noise propagation path. Winter conditions are the more interesting when system analysts are

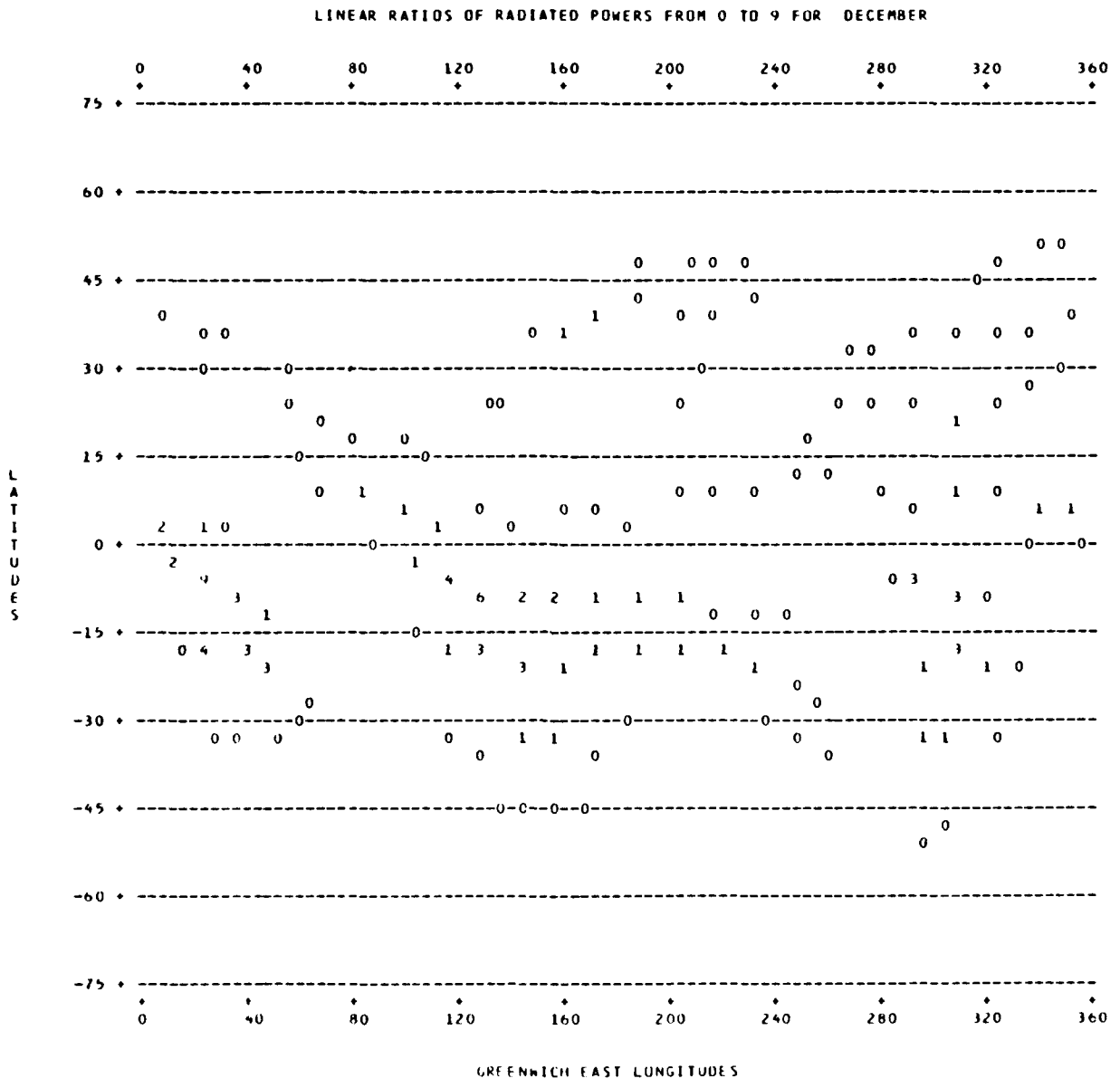

Figure 11. Locations of winter atmospheric noise radiation centroids.

concerned with maximum noise reduction due to a nuclear environment. For summer conditions (Figure 12) the noise sources tend to be located north of the equator (closer to the receiver sites) and the noise modeling now requires more propagation links.

Model Requirements

The modem models (References 3 and 4) require that the two following noise characteristics be specified:

1. Average noise amplitude, V_{ave} .
2. Ratio of the noise envelope rms to its average amplitude, V_d .

These two parameters are relatable to the two CCIR parameters (Reference 12). A third parameter Ψ , the ratio of the total noise power to the background Gaussian noise power, needs to be specified. Unfortunately, Ψ is not a CCIR parameter and is difficult to predict. Reference 3 provides an empirical relationship based on experimental data

$$\Psi(dB) = 2V_d(dB)\ \{1 - [1.049/V_d]^2\} \quad . \tag{4}$$

This relationship will be used until an improved prediction becomes available.

To satisfy these model requirements WEDCOM V will have at least two of the following options:

1. Specification of the receiver noise as was done for earlier WEDCOM versions. This option is useful for the cases where the major noise sources are local or are not due to thunderstorm activity. Minimum code computations are required.
2. User specification of the noise source locations, power and signal deviation.
3. Code selection of the noise sources based on user-specified season and diurnal data. This option requires a stored data base.

The V_{ave} and V_d parameters are available for each of these options. The first option requires the CCIR tables. A noise prediction model is required for the 2nd and 3rd options, to be executed as a separate activity from WEDCOM or as part of it.

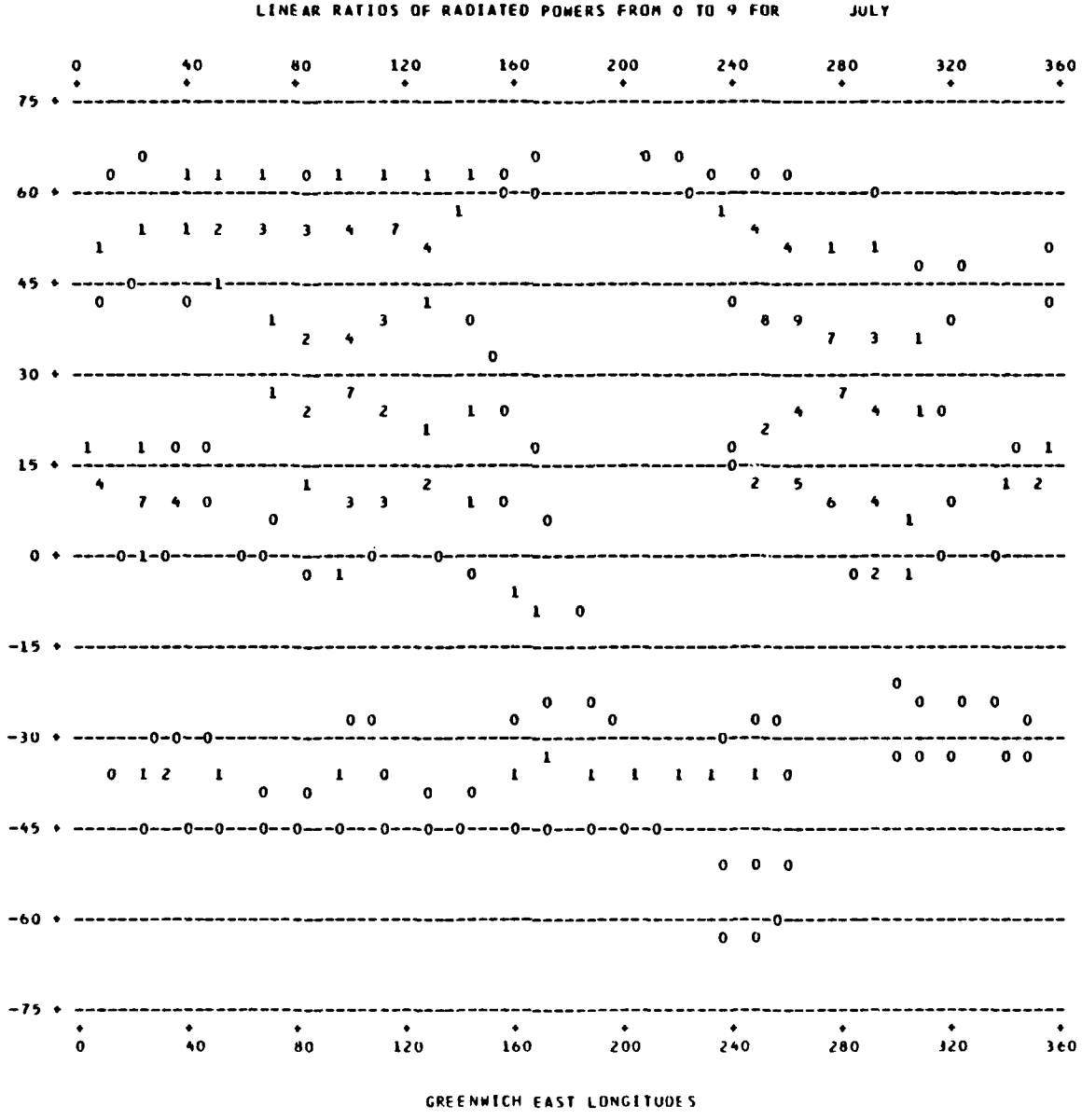

Figure 12. Locations of summer atmospheric noise radiation centroids.

Atmospheric Noise Prediction Model

An atmospheric noise prediction model was developed by the Westinghouse Georesearch Laboratory, WGL (Reference 13), and extended to include elevated receiver antennas by the Naval Research Laboratory, NRL (Reference 14). The WGL/NRL code was developed for VLF (10 to 30 kHz). A scaling factor developed by the Stanford Research Institute, SRI (Reference 15), extends the frequency range to include LF. The code predictions compare well with extensive worldwide atmospheric noise measurements for vertical polarization and with limited data for horizontally polarized signals received by elevated antennas. The horizontal noise component is related to anisotropic conversion from vertical to horizontal polarization at the receiver location only. The WEDCOM propagation models are more complete than the NRL models, and will consider quasi-TE (as well as quasi-TM) modes and ionospheric anisotropic effects along the entire propagation path. Thus, the horizontal received modes (especially important to A/C with trailing antennas) will receive a more complete evaluation. A limitation to the WGL/NRL code is that the noise source is assumed to be vertical. While this is thought to be the most dominant effect, some tests (see Reference 14) have shown that significant horizontal radiation can occur. More complete modeling, should it become available, will require little modification to WEDCOM to include the horizontal radiated component.

All noise sources cannot be individually evaluated by WEDCOM and an algorithm which will minimize the number is required. One available algorithm is found in the NRL code. The noise powers are combined into equivalent noise transmitters centered in 5-degree by 5-degree grids of the earth's surface. Where possible, the grids are further combined into 15-degree by 15-degree grids. A vector sum of the propagation modes (or rays) is not meaningful when utilizing this algorithm as the noise transmitter locations are centroids of many sources and the timing of all sources are statistically independent. WEDCOM will therefore only compute RMS values of the received noise.

Nuclear Environment V_{ave} and V_d Values

The prediction of V_{ave} in a nuclear environment is straightforward. Once the noise powers and locations have been specified, propagation links to the receiver can be evaluated and received noise powers determined.

The noise impulsivity parameter V_d is not easily estimated in a nuclear-disturbed environment. Two techniques have been used by analysts. An analytic

formulation is provided by Field and Lewenstein, Reference 16. The formulation is based on a single link uniform propagation path for the Gaussian background noise, and ignores any dispersive propagation changes. Impulsivity changes occur due to suppression or enhancement of the received background power.

A second formulation of the noise statistics was presented in Reference 3 for use with the modem models. For mathematical convenience the narrowband atmospheric noise is modeled as a modulated Gaussian random process, rather than the sum of impulsive and background noise components as was done in Reference 16. The impulsivity, V_d, is assumed to be unmodified by the nuclear environment.

Both models provide good comparisons to data, but a direct comparison for WEDCOM use is not easily determined, and an extensive effort for comparison is not warranted due to the lack of adequate modeling of Ψ (Equation 4).

Two methods of predicting V_d in a nuclear environment are presently under consideration. Each method is a variation of the two techniques mentioned above. In the first method V_d is estimated in the following manner:

1. Determine V_{ave}, V_d and Ψ for the normal environment.

2. Determine

$$A_G = \{V_{ave}(\text{disturbed})/V_{ave}(\text{normal})\}$$

$$A_I = \{V_I(\text{disturbed})/V_I(\text{normal})\}$$

where

V_I is the received signal strength from the nearest noise radiator.

3. Determine:

$$\Psi_d = \left(\frac{A_I}{A_G}\right)^2 \{\Psi - 1\} + 1$$

4. Determine V_d in disturbed environment by solving Equation 4 with the substitution of Ψ_d from Step 3 above.

The second method uses a variation of the V_d computation that is part of the WGL model:

1. The N most significant noise sources are determined in the undisturbed environment (V_{ave} is determined from these N sources). The locations, distances from the receivers, diurnal modifier index and transmitter powers are saved.

2. From the N sources, the propagation paths of a maximum of the five most significant transmitters are evaluated for both the normal and disturbed environments.
3. V_d is determined from the WGL algorithm (Reference 13), but with the received powers from Step 2, rather than the simplified estimates used in the WGL model.

Both methods will be evaluated and one will be implemented into WEDCOM V.

SIGNAL PROCESSING MODEL

The Stanford Research Institute (SRI) developed VLF/LF modem models (References 3 and 4) for the MEECN System Engineering Division of the Command and Control Technical Center (CCTC), Defense Communication Agency. These models estimate modem performance in an atmospheric noise environment, and have demonstrated a specific capability for predicting performance of selected MEECN modems. The model allows for a building block structure of simulating non-linear noise suppression devices (such as bandpass clippers and hard limiters) combined with various types of generic digital demodulators.

Figure 13 illustrates a simplified receiver block diagram that incorporates the individual building blocks of the SRI modem model. The receiver includes one of several available generic matched-filter models with or without a bandpass clipper. The clipping level of the bandpass clipper must be user specified. The input specifications and alternatives are listed in Table 10. The model outputs include the bit-error-rate (BER) and character-error-rate (CER), as listed in Table 11. The relationship between BER and CER assumes that the bit errors are independent. For an N-bit Baudot encoded character

$$CER = 1 - (1 - BER)^N \quad . \tag{5}$$

Error-correction is included as a user option, i.e., a 15/11 Hamming code whose code words are 15 bits in length and contain two teletype characters.

A working version of these models has been implemented, but as a separate activity from WEDCOM. Some model modifications were required and an integration scheme replaced. However, the basic model remains as originally implemented by SRI. Figure 14 illustrates an example execution. This case is for illustration and does not pertain to an existing system. The effects of limiters and a reduced

noise environment are shown (as could occur in a nuclear environment). The V_d = 1.049 dB curve corresponds to a Gaussian noise background where the improvements due to bandpass clippers are minimal.

Table 10. Modem model input specifications, options and mnemonics.

Definition	Modem Input
Pseudo-noise spread spectrum type	NO (none) CO (complementary) OR (orthogonal)
Modem type	PS (phase-shift key) MS (minimal shift key) CF (coherent frequency shift key) CS (compatible shift key) DC (differentially coherent PSK) NC (noncoherent frequency shift key)
Clipper in receiver?	YE (yes) NO (no)
Bit rate (per second)	0.<RATE≤1000.
V_d bandwidth (Hz)	0.<BWVD≤10000.
SNR bandwidth (Hz)	0.<BNSR≤100000.
Clipper bandwidth (Hz)	0.<BC≤5000.
Ratio of clipper saturation level in signal-to-noise rms level (dB)	-60.≤CSK≤60.
Processing loss due to mismatched filtering (dB)	0.≤LOSS≤10.
Noise impulsivity parameter, V_d (dB)	1.049≤VD≤25.
Signal-to-noise ratio value (dB)	-60.≤SNR≤40.

Table 11. Modem model output parameter definitions.

E_b/N_o	=	Bit-energy-to-noise-density ratio
BER	=	Bit-error-rate
BCER	=	Character-error-rate -- Baudot code
HCER	=	Character-error-rate -- Hamming 15/11 code
EFF	=	Clipper signal-to-noise ratio enhancement (dB)

Figure 13. Block diagram of simplified receiver model.

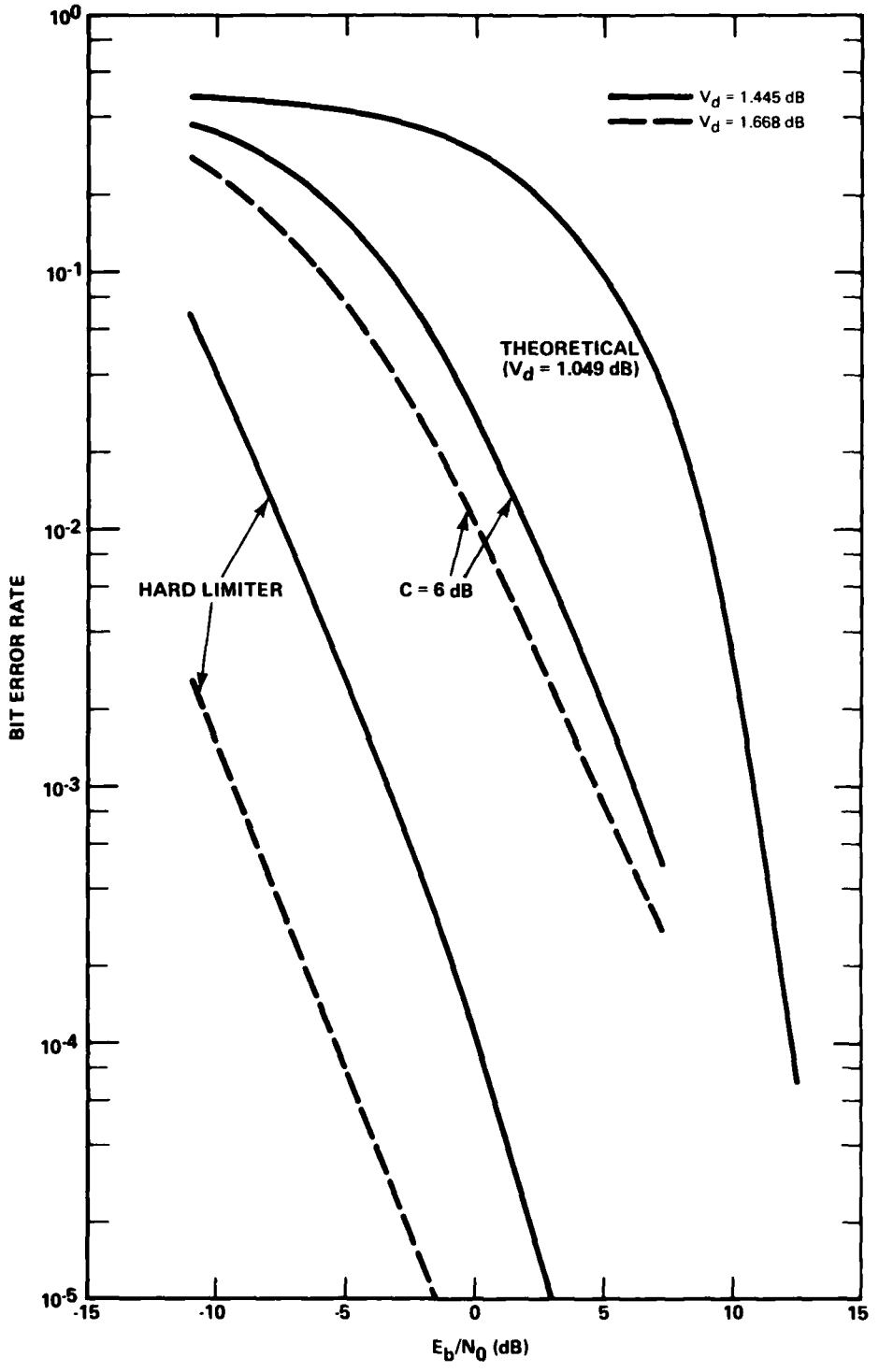

Figure 14. Noncoherent FSK for V_d = 1.049, 1.445, and 1.668 dB and two levels of bandpass clippers. Background noise has been reduced 4 dB.

REFERENCES

1. Rutherford, R.R., and W.S. Knapp, Status Report on Preparation of a Revised Longwave Communication Link Vulnerability Code, DNA 5869T, KT-81-022(R), Kaman Tempo, October 1981.

2. Rutherford, R.R., WEDCOM IV: A FORTRAN Code for the Calculation of ELF, VLF and LF Propagation in a Nuclear Environment, Volume 3, Computational Models, DNA 4422T-3, General Electric Company-TEMPO, November 1978.

3. Shohara, A., and C.K. Un, VLF/LF Modem Performance in Atmospheric Noise, Volume I, Stanford Research Institute, March 1977.

4. Bell, P.J., VLF/LF Modem Performance in Atmospheric Noise: User's Guide, Volume II, Stanford Research Institute, February 1977.

5. General Electric Company-TEMPO, Private Communication, WEPH VI: A FORTRAN Code for the Calculation of Ionization and Electromagnetic Propagation, 1976.

6. Knapp, W.S., Status Report on WEPH Code Modeling-1978, DNA 4688F, General Electric Company-TEMPO, November 1978.

7. Kaman Tempo, Private Communication, WESCOM: A FORTRAN Code for Evaluation of Nuclear Weapon Effects on Satellite Communications, 1981.

8. Morfitt, D.G., and C.H. Shellman, MODESRCH, An Improved Computer Program for Obtaining ELF/VLF/LF Mode Constants in an Earth-Ionosphere Waveguide, Interim Report No. 77T, Naval Electronics Laboratory Center, San Diego, CA, October 1976.

9. Booker, H.G., A Simplified Theory of ELF Propagation in the Earth-Ionosphere Transmission Line and Its Worldwide Applications, University of California, San Diego, March 1980.

10. Pappert, R.A., and L.R. Shockey, Ionospheric Reflection and Absorption Properties of Normal Modes at ELF, IR 772, NOSC, September 1977.

11. Wait, J.R., Electromagnetic Waves in Stratified Media, Pergamon Press, The McMillan Company, New York, 1962.

12. C.C.I.R., Documents of the Xth Planetary Assembly, Geneva, 1963, Report 322, ITU. Geneva 1964.

13. Maxwell, E.L., et al, Development of a VLF Atmospheric Noise Prediction Model, 70-942-VLFNO-R1, Westinghouse Georesearch Laboratory, June 1970.

14. Kelly, F., J.P. Hauser, F.J. Rhoads, Computer-Program Model for Predicting Horizontally and Vertically Polarized VLF Atmospheric Radio Noise at Elevated Receivers, NRL Report 8479, December 1981.

15. Gambill, B., Private Communication, Kaman Tempo.

16. Field, E.C., and M. Lewinstein, Amplitude-Probability Distribution Model for VLF/ELF Atmospheric Noise, IEEE Transactions on Communications, Vol. COM-26, No. 1, January 1978.

DISTRIBUTION LIST

DEPARTMENT OF DEFENSE

Assistant to the Secretary of Defense
Atomic Energy
ATTN: Executive Assistant

Defense Advanced Rsch Proj Agency
ATTN: GSD, R. Alewene
ATTN: STO, W. Kurowski

Defense Communications Agency
ATTN: Code 205
ATTN: Code 230
ATTN: J300 for Yen-Sun Fu

Defense Communications Engineer Center
ATTN: Code R410
ATTN: Code R123, Tech Lib
ATTN: Code R410, N. Jones

Defense Nuclear Agency
ATTN: RAAE, P. Lunn
ATTN: NATD
ATTN: STNA
ATTN: RAEE
ATTN: NAFD
ATTN: K. Schwartz
3 cy ATTN: RAAE
4 cy ATTN: STTI/CA

Defense Technical Information Center
12 cy ATTN: DD

Dep Under Secretary of Defense
Comm, Cmd, Cont & Intell
ATTN: Dir of Intelligence Sys

Field Command
Defense Nuclear Agency, Det 1
Lawrence Livermore National Lab
ATTN: FC-1

Field Command
Defense Nuclear Agency
ATTN: FCPR
ATTN: FCTXE
ATTN: FCTT, W. Summa

Interservice Nuclear Weapons School
ATTN: TTV

Joint Chiefs of Staff
ATTN: C3S
ATTN: C3S, Evaluation Office (HD00)

Joint Data Systems Support Ctr
ATTN: G510, G. Jones
ATTN: C-312, R. Mason
ATTN: C-500
ATTN: G510, P. Bird

National Security Agency
ATTN: W36, O. Bartlett
ATTN: B-3, F. Leonard

DEPARTMENT OF DEFENSE (Continued)

Joint Strat Tgt Planning Staff
ATTN: JLK, DNA Rep
ATTN: JLAA
ATTN: JPPFD
ATTN: JPSS
ATTN: JLKS
ATTN: JPTM

Under Secy of Def for Rsch & Engrg
ATTN: Strat & Theater Nuc Forces, B. Stephan
ATTN: Strategic & Space Sys (OS)

WWMCCS System Engineering Org
ATTN: J. Hoff

DEPARTMENT OF THE ARMY

Assistant Chief of Staff for Automation & Comm
ATTN: DAMO-C4, P. Kenny

BMD Advanced Technology Center
ATTN: ATC-R, D. Russ
ATTN: ATC-R, W. Dickinson
ATTN: ATC-T, M. Capps
ATTN: ATC-O, W. Davies

BMD Systems Command
ATTN: BMDSC-HLE, R. Webb
2 cy ATTN: BMDSC-HW

US Army Comm-Elec Engrg Instal Agency
ATTN: CC-CE-TP, W. Nair

US Army Communications Command
ATTN: CC-OPS-W
ATTN: CC-OPS-WR, H. Wilson

US Army Communications R&D Command
ATTN: DRDCO-COM-RY, W. Kesselman

US Army Materiel Dev & Readiness Cmd
ATTN: DRCLDC, J. Bender

USA Missile Command
ATTN: DRSMI-YSO, J. Gamble

DEPARTMENT OF THE NAVY

Joint Cruise Missiles Project Ofc
ATTN: JCMG-707

Naval Electronic Systems Command
ATTN: PME 106-4, S. Kearney
ATTN: Code 501A
ATTN: PME 117-211, B. Kruger
ATTN: Code 3101, T. Hughes
ATTN: PME-106, F. Diederich
ATTN: PME-117-2013, G. Burnhart
ATTN: PME 117-20

Naval Intelligence Support Ctr
ATTN: NISC-50

DEPARTMENT OF THE NAVY (Continued)

Naval Ocean Systems Center
ATTN: Code 532
ATTN: Code 5322, M. Paulson
ATTN: Code 5323, J. Ferguson

Naval Research Laboratory
ATTN: Code 4720, J. Davis
ATTN: Code 4700, S. Ossakow
ATTN: Code 4108, E. Szuszewicz
ATTN: Code 7500, B. Wald
ATTN: Code 6700
ATTN: Code 4700
ATTN: Code 4780
ATTN: Code 7950, J. Goodman
ATTN: Code 4187

Naval Surface Weapons Center
ATTN: Code F31

Naval Telecommunications Command
ATTN: Code 341

Office of Naval Research
ATTN: Code 414, G. Joiner
ATTN: Code 412, W. Condell

Strategic Systems Project Office
ATTN: NSP-43, Tech Lib
ATTN: NSP-2141
ATTN: NSP-2722

DEPARTMENT OF THE AIR FORCE

Air Force Geophysics Laboratory
ATTN: LYD, K. Champion
ATTN: OPR-1
ATTN: R. Babcock
ATTN: CA, A. Stair
ATTN: OPR, H. Gardiner
ATTN: PHY, J. Buchau
ATTN: R. O'Neil

Air Force Weapons Laboratory
ATTN: SUL
ATTN: NTN

Air University Library
ATTN: AUL-LSE

Assistant Chief of Staff
Studies & Analysis
ATTN: AF/SASC, C. Rightmeyer

Deputy Chief of Staff
Research, Development, & Acq
ATTN: AFRDQI

Deputy Chief of Staff
Plans and Operations
ATTN: AFXOKCD
ATTN: AFXOKT
ATTN: AFXOKS

Electronic Systems Div/SCT-2
ATTN: ESD/SCTE, J. Clark

Foreign Technology Division
ATTN: TQTD, B. Ballard
ATTN: NIIS Library

DEPARTMENT OF THE AIR FORCE (Continued)

Rome Air Development Center
ATTN: OCS, V. Coyne
ATTN: OCSA, R. Schneible
ATTN: TSLD

Rome Air Development Center
ATTN: EEP, J. Rasmussen
ATTN: EEPS, P. Kossey

Strategic Air Command
ATTN: ADWA
ATTN: DCX
ATTN: XPQ
ATTN: XPFC
ATTN: DCZ
ATTN: NRI/STINFO Library
ATTN: XPFS

OTHER GOVERNMENT AGENCIES

Department of Commerce
National Bureau of Standards
ATTN: Sec Ofc for R. Moore

Department of Commerce
National Oceanic & Atmospheric Admin
ATTN: R. Grubb

Institute for Telecommunications Sciences
ATTN: A. Jean
ATTN: L. Berry
ATTN: W. Utlaut

NATO

NATO School (SHAPE)
ATTN: US Documents Officer

DEPARTMENT OF ENERGY CONTRACTORS

University of California
Lawrence Livermore National Lab
ATTN: L-31, R. Hager
ATTN: Tech Info Dept Library

Los Alamos National Laboratory
ATTN: T. Kunkle, ESS-5
ATTN: D. Simons
ATTN: MS 664, J. Zinn
ATTN: MS 670, J. Hopkins
ATTN: R. Jeffries
ATTN: J. Wolcott
ATTN: P. Keaton

Sandia National Laboratories
ATTN: T. Cook
ATTN: B. Murphey

Sandia National Laboratories
ATTN: Org 1250, W. Brown
ATTN: Org 4231, T. Wright
ATTN: Space Project Div
ATTN: D. Thornbrough
ATTN: Tech Lib 3141
ATTN: D. Dahlgren

DEPARTMENT OF DEFENSE CONTRACTORS (Continued)

BDM Corp
ATTN: L. Jacobs
ATTN: T. Neighbors

Berkeley Rsch Associates, Inc
ATTN: S. Brecht
ATTN: J. Workman
ATTN: C. Prettie

University of California at San Diego
ATTN: H. Booker

Computer Sciences Corp
ATTN: F. Eisenbarth

EOS Technologies, Inc
ATTN: W. Lelevier
ATTN: B. Gabbard

GTE Communications Products Corp
ATTN: R. Steinhoff

GTE Communications Products Corp
ATTN: J. Concordia
ATTN: I. Kohlberg

Institite for Defense Analyses
ATTN: H. Gates
ATTN: J. Aein
ATTN: E. Bauer
ATTN: H. Wolfhard

Johns Hopkins University
ATTN: C. Meng
ATTN: K. Potocki
ATTN: J. Phillips
ATTN: T. Evans
ATTN: J. Newland
ATTN: P. Komiske

Kaman Sciences Corp
ATTN: E. Conrad

Kaman Tempo
ATTN: B. Gambill
ATTN: DASIAC
ATTN: W. Schuleter
ATTN: W. McNamara
2 cy ATTN: W. Knapp
2 cy ATTN: R. Rutherford

Kaman Tempo
ATTN: DASIAC

Maxim Technologies, Inc
ATTN: E. Tsui
ATTN: J. Marshall
ATTN: R. Morganstern

Mitre Corp
ATTN: G. Harding
ATTN: A. Kymmel
ATTN: MS J104/M, R. Dresp
ATTN: C. Callahan

Science Applications, Inc
ATTN: M. Cross

DEPARTMENT OF DEFENSE CONTRACTORS (Continued)

Mission Research Corp
ATTN: R. Bigoni
ATTN: G. McCartor
ATTN: F. Guigliano
ATTN: F. Fajen
ATTN: D. Knepp
ATTN: Tech Library
ATTN: R. Kilb
ATTN: R. Bogusch
ATTN: R. Hendrick
ATTN: C. Lauer
ATTN: S. Gutsche
ATTN: R. Dana

Mitre Corp
ATTN: W. Hall
ATTN: J. Wheeler
ATTN: W. Foster
ATTN: M. Horrocks

Pacific-Sierra Research Corp
ATTN: F. Thomas
ATTN: H. Brode, Chairman SAGE
ATTN: E. Field, Jr

Physical Research, Inc
ATTN: R. Deliberis
ATTN: J. Devore
ATTN: T. Stephens
ATTN: J. Thompson

R&D Associates
ATTN: R. Turco
ATTN: M. Gantsweg
ATTN: C. Greifinger
ATTN: F. Gilmore
ATTN: H. Ory
ATTN: G. Stcyr
ATTN: W. Karzas
ATTN: W. Wright
ATTN: P. Haas

Rockwell International Corp
ATTN: R. Buckner

Rockwell International Corp
ATTN: S. Quilici

SRI International
ATTN: A. Burns
ATTN: G. Price
ATTN: R. Tsunoda
ATTN: J. Vickrey
ATTN: V. Gonzales
ATTN: D. Neilson
ATTN: J. Petrickes
ATTN: M. Baron
ATTN: R. Livingston
ATTN: D. McDaniels
ATTN: W. Chesnut
ATTN: G. Smith
ATTN: C. Rino
ATTN: W. Jaye
ATTN: R. Leadabrand

END

FILMED

1-85

DTIC